

pubs.acs.org/joc Article

# $\delta$ -Azaproline and Its Oxidized Variants

Yassin M. Elbatrawi, Kyle P. Pedretty, Nicole Giddings, H. Lee Woodcock, and Juan R. Del Valle\*



Cite This: J. Org. Chem. 2020, 85, 4207-4219



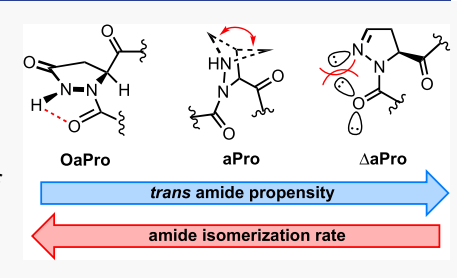
**ACCESS** 

III Metrics & More

Article Recommendations

s Supporting Information

**ABSTRACT:** Peptides featuring backbone N-amino substituents exhibit unique conformational properties owing to additional electrostatic, hydrogen-bonding, and steric interactions. Here, we describe the synthesis and conformational analysis of three  $\delta$ -azaproline derivatives as potential proline surrogates. Our studies demonstrate stereoelectronic tuning of heterocyclic ring pucker, *cis/trans* amide propensity, and amide isomerization barriers within a series of oxidation state variants. A combination of NMR, X-ray diffraction, and density functional theory calculations shows that electron density and hybridization at the  $\delta$  position play a dominant role in the conformational preferences of each analogue. Both  $\delta$ -azaproline and  $\gamma$ , $\delta$ -dehydro- $\delta$ -azaproline exhibit



strong *trans* amide rotamer propensities irrespective of ring conformation, while a novel residue,  $\gamma$ -oxo- $\delta$ -azaproline, features rapid amide isomerization kinetics and isoenergetic amide bond geometries influenced by torsional strain and H-bonding interactions. The introduction of the  $\delta$  heteroatom in each residue allows the decoupling of structural effects that are typically linked in proline and its pyrrolidine-substituted analogues.  $\delta$ -Azaproline derivatives thus represent useful probes of prolyl amide isomerism with potential applications in peptidomimetic drug design and protein folding.

## 1. INTRODUCTION

Proline is unique among the canonical proteinogenic amino acids because of its backbone torsional rigidity and the tertiary amide it forms when incorporated into peptides. These amides exhibit an unusually high propensity to adopt the energetically disfavored cis conformation. Analyses of protein structural databases reveal that approximately 6% of prolyl amide bonds exist as the cis rotamer, whereas non-prolyl cis amides are encountered at a frequency less than 0.05%.1 The isomerization of proline amide bonds is the rate-determining step in the folding of several proteins and is known to be catalyzed by a family of therapeutically relevant enzymes.2 The incorporation of unnatural proline surrogates has also revealed the importance of prolyl amide bond geometry for the function of several proteins.<sup>3</sup> Although replacement of proline with acyclic residues can enforce a  $180^{\circ}$   $\omega$  dihedral angle, this approach compromises the rigidity of native  $\phi$  and  $\psi$  backbone torsions. Conversely, non-peptidic "locked" amide isosteres preclude isomerization altogether and may deviate considerably from proline-like  $\phi$  and  $\psi$  dihedral angles. Constrained proline analogues with fast amide isomerization kinetics and enhanced trans amide propensity are thus desirable for use as conformational probes in structure-function studies and models of protein folding.

Designed proline analogues often feature pyrrolidine ring substituents, alterations to the ring size or polycyclic covalent constraints across two or more residues to impart conformational bias. A particularly well-studied series of analogues are those harboring electron-withdrawing heteroatoms at the  $\gamma$  position. These residues are synthetically accessible from naturally abundant (R)-4-hydroxyproline (Hyp) and exploit

the gauche effect to influence the ring conformation (Figure 1). The resulting changes in ground-state energies for endo-/exo-puckered conformers can lead to strong enhancement of trans-amide population via a stabilizing  $n \rightarrow \pi^*$  interaction. Incorporation of a second heteroatom within the 5-membered ring can likewise exert pronounced effects on the backbone dihedral angles and amide geometry. For example,  $\gamma$ -thiaproline and  $\gamma$ -oxaproline exhibit lower barriers to amide isomerization and enhanced cis amide populations relative to Pro. A similar enhancement of cis rotamer population was recently observed for  $\gamma$ -azaproline, while the conformational characteristics of  $\gamma$ -(dimethylsila)proline closely mimic those of Pro.  $\alpha$ -Azaproline, which harbors a stereodynamic  $\alpha$  center, was recently accommodated within a well-folded all-trans collagen model system without significant energetic penalty.

We perceived a need for isosteric replacements that uncouple amide rotamer propensity from ring puckering and other canonical stabilizing interactions within prolyl peptides. Given our interest in N-heteroatom-substituted peptides, we chose to investigate the conformational properties of  $\delta$ -azaproline (aPro) as well as its oxidized derivatives  $\gamma$ ,  $\delta$ -dehydro- $\delta$ -azaproline ( $\Delta$ aPro) and  $\gamma$ -oxo- $\delta$ -azaproline (OaPro). As depicted in Figure 1, these derivatives may leverage stereoelectronic effects distinct to those typically

Received: December 16, 2019 Published: February 26, 2020



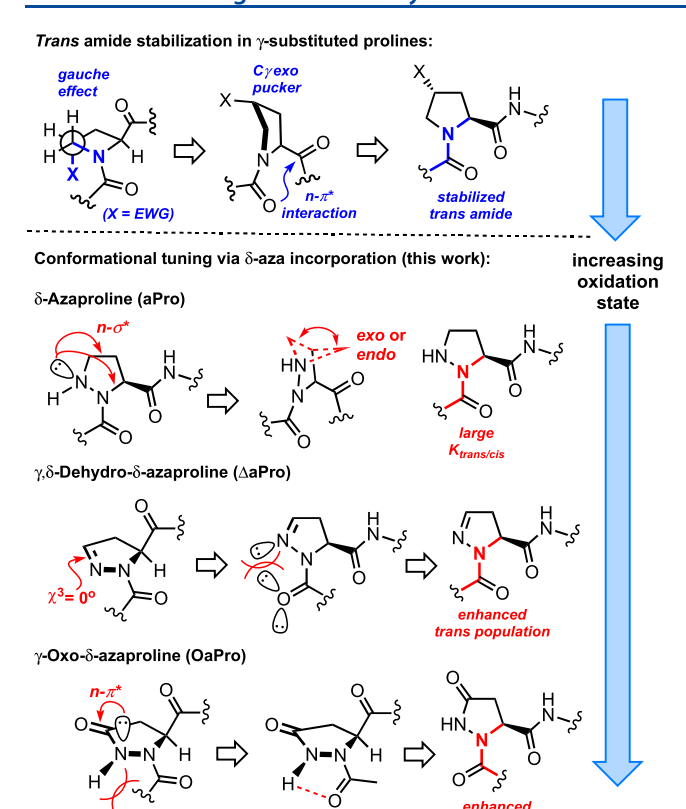


Figure 1. Canonical *trans* amide stabilization model for Pro and conformational features of δ-azaproline variants.

invoked in *trans* amide-based  $\gamma$ -substituted analogues. We previously observed that backbone N-amination of non-prolyl residues within peptides results in maintenance of *trans* amide bond geometry despite the presence of an amide substituent. This is in contrast to N-alkylation, which results in significant *cis* amide population. Our group and others have attributed this to strong electronic repulsion between lone pairs on the N-amino substituent and the amide carbonyl in the *cis* configuration,  $^{10a,11}$  Importantly, this effect persists under physiological conditions because the N-amino group remains unprotonated above  $\sim$ pH 2.  $^{10a,12}$  We expected that a similar effect would manifest in aPro, whereas N $\delta$  lone pair delocalization into the neighboring bonds may give rise to distinct conformational preferences in  $\Delta$ aPro and OaPro.

The sp<sup>2</sup> character of the  $\gamma$  and  $\delta$  atoms in  $\Delta$ aPro and OaPro was also viewed as an attractive structural feature to probe the importance of ring puckering on amide configuration. Proline "flattening" has previously been achieved through the introduction of unsaturation into the ring or by fusion to a cyclopropane ring. The presence of these flattened derivatives in the anti-diabetic drug saxigliptin (Onglyza), peptidomimetic clinical candidates, biologically active natural products, and folded peptides and proteins active natural products, their broad utility as noncanonical proline surrogates. Similar to methano- and dehydroprolines,  $\Delta$ aPro and OaPro feature  $\chi^3$  dihedral angles locked at 0°. The acyl hydrazines in these surrogates may also engage in favorable intermolecular interactions that are not available to their carbon-based analogues.

Here, we describe the conformational analysis of aPro and its oxidized variants. As part of this study, we developed a novel synthesis of aPro derivatives via electrophilic amination and late-stage ring formation. This approach allows, for the first time, the incorporation of  $\delta$ -aza analogues of proline into host peptides on a solid support. Analysis by density functional theory (DFT) calculations, NMR, and X-ray diffraction demonstrates divergent conformational characteristics that are highly dependent on the electron density and hybridization at the  $\delta$  position. Trends within this series of analogues support the role of electronic effects on the thermodynamics and kinetics of peptide-bond isomerization and inform the use of aPro derivatives in the design of biologically active and well-folded peptide mimics.

#### 2. RESULTS

The conformation of peptides harboring the aPro residue has been the subject of two recent studies. <sup>18</sup> In both, N-acylated aPro derivatives exhibited the presence of only a single amide rotamer by NMR over a range of temperatures. Subsequent NMR and Fourier-transform infrared spectroscopy studies led to the suggestion that aPro amides exist exclusively in the *cis* configuration. This interpretation was puzzling given our experience with acyclic N-amino peptides<sup>10a</sup> as well as experimental and computational data from the 6-membered homologue of aPro, piperazic acid (Piz). <sup>19</sup> Ciufolini and coworkers employed semiempirical methods to calculate the *cis* amide rotamer of Ac-Piz-OMe to be over 3.5 kcal/mol higher in energy than the *trans*, which is consistent with the unusual conformational homogeneity of Piz derivatives on the NMR time scale relative to pipecolic acid. A strong preference for the *trans* rotamer was also calculated for Ac-ΔaPro-OMe. <sup>19a</sup>

Although crystalline solids are subject to packing forces that can influence conformation, the absence of cis amide rotamers in existing crystal structures of acylated Piz,  $\Delta a Pro$ , or aPro residues is notable. We surveyed the CCDC structural database and found 22 deposited N-acyl Piz structures all of which exhibit the trans amide geometry N-terminal to Piz even within peptide macrocycles. One N-acyl  $\Delta a Pro$  and two N-acyl aPro solid-state structures were also identified, each featuring trans amide bonds. Interestingly, X-ray diffraction of an aProcontaining macrocyclic peptide was reported by Sinha and coworkers as part of a study that assigns the aPro cis amide as the energetically favored rotamer in solution. A trans-substantiating effect for  $\delta$  heteroatoms is further supported by studies on  $\delta$ -oxaproline derivatives that adopt a single trans rotamer in solution.

We prepared acetyl methyl esters of aPro,  $\Delta$ aPro, and OaPro to investigate thermodynamic stability and kinetics of amide bond isomerization. Previous syntheses of optically active aPro from malic acid and  $\alpha$ -hydroxy- $\gamma$ -butyrolactone rely on  $S_N2$ displacement at the  $\alpha$  carbon using hydrazine-based nucleophiles.<sup>22</sup> A chiral auxilliary-mediated dipolar cycloaddition approach to  $\Delta$ aPro has also been described, affording enantiopure products following diastereomeric resolution and hydrolysis of the auxiliary.<sup>23</sup> As shown in Scheme 1, we developed a novel N-N bond formation approach starting from readily available (O-TBS)-L-homoserine methyl ester (1).<sup>24</sup> Electrophilic amination of 1 using 2-(t-butyl)-3,3-(diethyl)-oxaziridine-2,3,3-tricarboxylate (TBDOT)<sup>10b,25</sup> followed by acetylation afforded ( $N\delta$ -Boc)-protected  $\alpha$ -hydrazino ester 2 in 68% yield over two steps. Direct chlorination of the silyl ether with triphenylphosphine dichloride<sup>26</sup> was followed by base-promoted cyclization and Boc deprotection to give aPro derivative 3. Oxidation to the  $\Delta$ aPro analogue 4 was achieved by treating 3 with I<sub>2</sub>/Et<sub>3</sub>N in DCM. The OaPro

Scheme 1. Synthesis of Enantiopure Acetylated aPro, ΔaPro, and OaPro Monomers

$$\begin{array}{c} \text{OTBS} \\ \text{OTBS} \\ \text{OTBS} \\ \text{OCO}_2\text{Et} \\ \text{NaHCO}_3, \text{ H}_2\text{O:THF} \\ \text{2) AcCI,NaHCO}_3, \text{ DCM} \\ \text{1} \\ \text{CO}_2\text{Me} \\ \text{1} \\ \text{CO}_2\text{Me} \\ \text{1} \\ \text{0} \\$$

derivative **6** was prepared from N-amino aspartic acid diester **5**, which is obtained in one step from commercially available H-Asp(tBu)-OMe·HCl.<sup>10b</sup> Acetylation and tandem acidolysis/cyclization using SOCl<sub>2</sub> and water afforded **6** in 44% yield.<sup>27</sup>

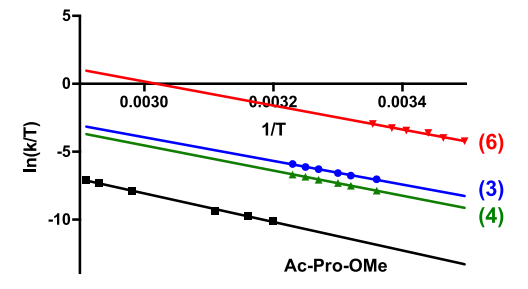
With the acetyl monomers in hand, we examined trans/cis amide equilibria by <sup>1</sup>H NMR in CDCl<sub>3</sub> and D<sub>2</sub>O (Table 1).

Table 1. Trans/cis Equilibrium Constants for aPro Analogues Obtained from <sup>1</sup>H NMR in CDCl<sub>3</sub> and D<sub>2</sub>O

compound	$K_{trans/cis}$ (CDCl <sub>3</sub> )	$K_{trans/cis}$ (D <sub>2</sub> O)
Ac-Pro-OMe	3.6	4.5
Ac-aPro-OMe (3)	>99	12
Ac- $\Delta$ aPro-OMe (4)	>99	44
Ac-OaPro-OMe (6)	0.5	0.8

Both aPro and  $\Delta$ aPro derivatives 3 and 4 exist as a single rotamer in CDCl<sub>3</sub> at rt. The control compound, Ac-Pro-OMe, exhibits a characteristic nuclear Overhauser effect (NOE) correlation between H $\alpha$  and the acetyl methyl protons in the *cis* rotamer, which is largely absent in the *trans* form. This correlation was also largely absent in the 1D NOE spectra of 3 and 4 in CDCl<sub>3</sub> upon irradiation of the H $\alpha$  signal, suggesting a *trans* amide geometry. A small population of the *cis* rotamers of 3 and 4 was evident in D<sub>2</sub>O. This is consistent with attenuation of electrostatic lone pair repulsive effects upon switching to a solvent with a higher dielectric constant. The major rotamer of Ac-OaPro-OMe (6) in both solvents was assigned *cis* based on the presence of the diagnostic H $\alpha$ -Me<sub>Ac</sub> NOE correlation. Like Ac-Pro-OMe, the equilibrium shifted more toward the *trans* rotamer of 6 in D<sub>2</sub>O.

Rate constants for amide bond isomerization in  $D_2O$  were determined by conducting a series of 1D  $^1H$  saturation-transfer NMR experiments at various temperatures. Eyring plots were generated to compare the activation parameters ( $\Delta H^{\ddagger}$  and  $\Delta S^{\ddagger}$ ) for the lower energy conformers of 3, 4, and 6 relative to Ac-Pro-OMe (Figure 2). The free-energy barriers to isomer-



**Figure 2.** Eyring plots for aPro variants in  $D_2O$ .

ization (Table 2) are mainly enthalpic in origin and are all significantly lower than that of Ac-Pro-OMe. Such lowering can be attributed to the strong inductive effect imposed by the added heteroatom, leading to an overall decrease in the double bond character of the amide bond.

We next sought to gain more insights into conformational preferences and relevant stereoelectronic effects from computational methods. DFT calculations at the  $\omega$ -B97X-D/6-31+G\*\* level of theory were carried out with the SM8 implicit water solvation method on Ac-Pro-OMe, 3, 4, and 6. The pyrrolidine ring of proline is known to adopt two main puckers at the  $\gamma$  carbon, exo and endo. Geometry optimizations were thus carried out on four conformers of the aPro analogue 3 (cis and trans of the C $\gamma$  exo and C $\gamma$  endo puckers). Two conformers of the flattened proline analogues 4 and 6 were considered (cis and trans amide geometry). Ac-aPro-OMe (3) favored the *trans* amide in both  $C\gamma$  exo and endo forms by 3.8 and 4.7 kcal/mol, respectively (Figure 3). Both energy gaps are significantly higher than those calculated for Ac-Pro-OMe, consistent with the pronounced trans amide bias observed by NMR. Unlike Ac-Pro-OMe, analogue 3 exhibited a preference for the exo pucker in the cis amide conformation.

Figure 4 depicts the energy minimized conformations of *cis* and *trans* Ac- $\Delta$ aPro-OMe (4). Both conformers exhibit a planar dihydropyrazole ring, with the *trans* amide rotamer favored by 4.3 kcal/mol. The higher overall  $\Delta E_{cis/trans}$  value for 4 relative to aPro derivative 3 is consistent with the higher *trans*-propensity observed by NMR (see Table 1). The periplanar relationship between the N-N and C=O<sub>Ac</sub> bonds suggests a particularly strong electrostatic repulsion between lone pairs on nitrogen and oxygen in the *cis* conformer of 4.

The oxidized OaPro derivative 6 was calculated to favor the cis amide conformer by 2.0 kcal/mol (Figure 5). Although designed as a flattened Pro analogue, the pyrazolidinone ring in **6** deviates slightly from planarity in both amide conformations. The presence of the hydrogen substituent on N $\delta$  distinguishes **6** from  $\Delta$ aPro derivative **4** and introduces a potential 1,3 steric interaction between the NH and acetyl methyl group. While the N-H and C=O<sub>Ac</sub> bonds are nearly synperiplanar in the cis amide conformer of 6, the acetyl methyl group in the trans configuration avoids this interaction through a more pronounced twist in the N-N bond. Increased planarity in the cis conformer suggests the presence of an intramolecular C5 H-bond. The presence of a N $\delta$ H···O bond in *cis-6* is further supported by the previously observed increase in trans amide population when shifting to a more polar solvent (see Table 1).

The energy minimized structures of 3 and 4 revealed main chain torsions consistent with proline in PPII-type helices. Therefore, we conducted NBO analysis to identify potential

Table 2. Activation Parameters for trans/cis Amide Isomerization of aPro Variants in D<sub>2</sub>O<sup>a</sup>

compound	$\Delta H^{\ddagger}$ (kcal/mol)	$\Delta S^{\ddagger}$ [(cal/mol·K)]	$\Delta G^{\ddagger}$ (kcal/mol)	$k(25  {}^{\circ}\text{C})  (s^{-1})$
Ac-Pro-OMe	$20.8 \pm 0.6$	$-0.8 \pm 1.8$	$21.0 \pm 0.8$	0.002
Ac-aPro-OMe (3)	$17.3 \pm 0.6$	$-3.2 \pm 2.1$	$18.3 \pm 0.9$	0.266
Ac- $\Delta$ aPro-OMe (4)	$18.4 \pm 0.4$	$-1.1 \pm 1.2$	$18.7 \pm 0.5$	0.122
Ac-OaPro-OMe (6)	$17.6 \pm 1.0$	$5.9 \pm 3.4$	$15.8 \pm 1.4$	15.64
<sup>a</sup> All values correspond to trans-	→ cis activation barriers with	the exception of <b>6</b> ( $cis \rightarrow trans$ )	).	

 $\frac{\Delta E_{cis-trans} =}{4.7 \text{ kcal/mol}}$   $trans-a \text{Pro}_{endo}$   $\frac{\Delta E_{endo-exo} =}{0.0 \text{ kcal/mol}}$   $\frac{\Delta E_{endo-exo} =}{0.9 \text{ kcal/mol}}$   $\frac{\Delta E_{cis-trans} =}{3.8 \text{ kcal/mol}}$   $cis-a \text{Pro}_{endo}$ 

Figure 3. Low-energy conformers of Ac-aPro-OMe (3) from DFT calculations ( $\omega$ -B97X-D/6-31+G\*\*, implicit solvent = H<sub>2</sub>O).

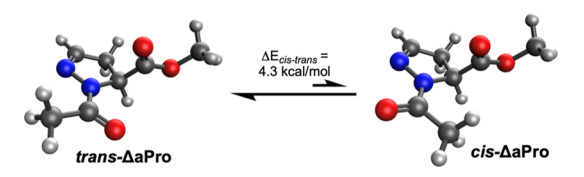


Figure 4. Low-energy conformers of Ac-ΔaPro-OMe (4) from DFT calculations (ω-B97X-D/6-31+G\*\*, implicit solvent = H<sub>2</sub>O).

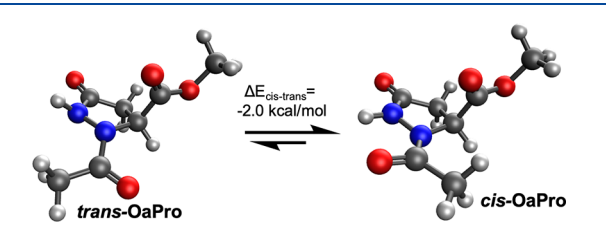


Figure 5. Low-energy conformers of Ac-OaPro-OMe (6) from DFT calculations ( $\omega$ -B97X-D/6-31+G\*\*, implicit solvent = H<sub>2</sub>O).

 $n{ o}\pi^*$  interactions between the acetyl carbonyl oxygen donor and the ester carbonyl carbon acceptor orbitals, as this has been shown to stabilize *trans* amide bonds within folded peptides and proteins (Table 3). St. Interestingly, aPro *trans*- $3_{\rm endo}$  showed a 1.18 kcal/mol stronger  $n{ o}\pi^*$  interaction than *trans*- $3_{\rm exo}$ , which was in contrast to *trans*-Ac-Pro-OMe where the exo pucker is associated with a stronger  $n{ o}\pi^*$  overlap.

Moreover, the main chain torsions ( $\phi$  and  $\psi$ ) in trans-3 $_{\rm endo}$  resembled those in trans-Ac-Pro-OMe $_{\rm exo}$ , whereas those in trans-3 $_{\rm exo}$  more closely mimicked trans-Ac-Pro-OMe $_{\rm endo}$ . Further inspection of hyperconjugative interactions in trans-3 revealed strong delocalization of the N $\delta$  lone pair electrons into the neighboring N-C $\alpha$  and C $\gamma$ -C $\beta$   $\sigma^*$  orbitals (~12 kcal/mol stabilization in both puckered conformers). The calculated  $\phi$  torsions in the endo and exo puckered forms of trans-3 maximize this delocalization and are dominant factors in the conformational preferences of the pyrazolidine ring.

Compound *trans*-4 exhibited a modest  $n\rightarrow\pi^*$  interaction of 0.75 kcal/mol while *trans*-6 did not show any appreciable overlap. Consistent with established trends for Ac-Pro-OMe, stronger  $n\rightarrow\pi^*$  interactions correlated well with shorter distances between the amide carbonyl oxygen and the ester carbonyl carbon and with more acute  $\phi$  and  $\psi$  dihedral angles in the aPro analogues. Notably, computed amide bond resonance energies for *trans*-Ac-Pro-OMe<sub>exo</sub>, *trans*-3<sub>exo</sub>, *trans*-4, and *cis*-6 are 99.8, 75.3, 83.0, and 62.8 kcal/mol, respectively, which correlates with our experimental isomerization free energy barriers (see Table 2).

X-ray diffraction of crystalline aPro derivatives provided additional insights into conformation. The structure of OaPro 6 exhibits a *cis* amide bond geometry in the solid state. The  $\phi$  and  $\psi$  torsions in 6 (–89 and 169°, respectively) are more extended than those typically observed for proline (Figure 6).<sup>2d</sup> The NH also appears to engage in the aforementioned

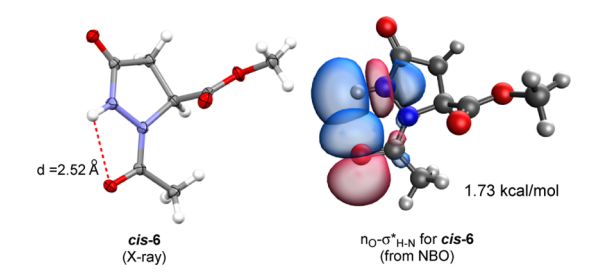
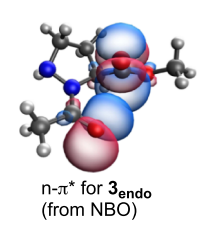


**Figure 6.** X-ray crystal structure and NBO analysis of *cis*-**6** depicting a C5 H-bond.

C5 hydrogen bond with the acetyl carbonyl O. The strength of this interaction was estimated to be 1.73 kcal/mol ( $n_O \rightarrow$ 

Table 3. Computed trans Amide Rotamer  $n\rightarrow\pi^*$  Interactions from NBO Analysis

compound	n-π*	τ	d	ф	Ψ
compound	(kcal/mol)	(°)	(Å)	(°)	(°)
	(KCal/IIIOI)	()	(A)	()	()
Ac-Pro-OMe <sub>endo</sub>	0.64	94.9	3.05	-68.1	156.7
Ac-Pro-OMe <sub>exo</sub>	1.81	94.3	2.87	-57.0	148.2
Ac-aPro-OMe(3) <sub>endo</sub>	1.60	92.9	2.88	-51.6	146.6
Ac-aPro-OMe(3) <sub>exo</sub>	0.42	98.0	3.15	-77.6	155.9
Ac-ΔaPro-OMe( <b>4</b> )	0.75	90.5	3.02	-62.0	160.0
Ac-Oxo-aPro-OMe(6	i) < 0.1	98.8	3.60	-108.6	172.5



 $\sigma^*_{\mathrm{H-N}}$ ) from NBO calculations. As shown in Figure 5 above, the energy minimized conformation of *trans-6* features pyramidalization of the amide N in order to avoid a 1,3 steric clash between the NH and acetyl methyl group. The X-ray structure of *cis-6* is in excellent agreement with the computed structure, exhibiting near-planarity of the acetyl N.

Although attempts to crystallize 3 from a variety of solvents were unsuccessful, a benzylated glycyl dipeptide derivative provided diffraction quality crystals upon dissolution in hot  $CHCl_3$  and slow evaporation. To our surprise, these conditions resulted in the oxidation of the pyrazolidine ring to give 7, suggesting that air oxidation of aPro residues may also occur readily at rt (Figure 7). Indeed, we found that prolonged

Figure 7. X-ray crystal structure of trans-7.

storage of Ac-aPro-Gly-OBn or compound 3 at rt resulted in significant amounts of the  $\Delta a$ Pro derivatives detectable by  $^1$ H NMR. The  $\Delta a$ Pro residue in the X-ray structure of 7 closely matches that derived from computation. This includes apparent  $n \rightarrow \pi^*$  delocalization with a donor—acceptor distance of 2.97 Å and a bond trajectory  $(\tau)$  of 93.2° as well as  $\phi$  and  $\psi$  torsions of -60 and  $151^\circ$ , respectively. These results show that  $\Delta a$ Pro can engage in proline-like stereoelectronic interactions despite its unpuckered nature.

We next developed an Fmoc-based solid-phase protocol for the synthesis of peptides harboring  $\Delta a Pro$  and Oa Pro. Dipeptide precursors to aPro and  $\Delta a Pro$  residues were synthesized in solution starting from H-Hse(TBS)-OBn, while those for OaPro were synthesized from H-Asp(tBu)-OBn (Scheme 2). N-Amination of the amino esters with

Scheme 2. Synthesis of Orthogonally Protected *N*-Amino Dipeptides for SPPS

TBDOT was followed by condensation with Fmoc-protected amino acid chlorides to afford 8a-d in good yields. Hydrogenolysis provided the requisite free acids 9a-d for use in SPPS.

We selected a 4-residue peptide as well as an 8-residue type II'  $\beta$ -hairpin model developed by Balaram and co-workers as host sequences for Pro mutation. Peptide elongation was carried out on a Rink amide MBHA resin using a standard Fmoc-based strategy and HCTU/NMM activation. Target sequences harboring aPro or  $\Delta$ aPro were prepared via on-resin

silyl ether cleavage with TBAF, heterocycle formation under Mitsunobu conditions (PPh<sub>3</sub>/DIAD), and acid-mediated cleavage from the resin (Scheme 3). Analysis of the crude

Scheme 3. Solid-Phase Synthesis of  $\Delta a$ Pro-Containing Peptides

material showed significant amounts of  $\Delta a Pro$  derivatives 12 in addition to 11. The oxidative decomposition of 11 was sufficiently rapid so as to preclude the isolation of pure aPro peptides. The yields of 12 could be increased by the treatment of semi-crude 11 with aqueous  $H_2O_2$ .

Peptides harboring OaPro residues were prepared by elaboration of *N*-amino dipeptides **9c** and **9d** as shown in Scheme 4. We found that acid-mediated cyclization to form the pyrazolidinone ring occurred in tandem with Boc deprotection and cleavage from the resin. OaPro-containing peptides **13a** 

Scheme 4. Solid-Phase Synthesis of OaPro-Containing Peptides

and 13b were thus obtained in 43 and 46% overall yield following purification by RP-HPLC.

Peptides 12 and 13 were obtained as diastereomerically pure compounds by both <sup>1</sup>H NMR and analytical RP-HPLC. Because our approach relies on incorporation of a dipeptide fragment that may be susceptible to racemization, we sought to further confirm the integrity of the hydrazino acid  $\alpha$  carbon following condensation. We thus amidated Fmoc-Gly-Hse-(TBS)-OH with (R)- $\alpha$ -methylbenzylamine and found the d.r. of the crude product to be  $\geq 27:1$  by <sup>1</sup>H NMR.<sup>30</sup> Given the known proclivity for N-methyl peptide fragments to undergo significant epimerization during C-terminal condensation, 32 we hypothesize that the electron-withdrawing N-amino substituent in dipeptides such as 9 confers resistance to racemization. This is likely due to the reduced nucleophilicity of the acetyl carbonyl oxygen and suppressed formation of the racemization-prone oxazolonium intermediate. Our dipeptide-based synthetic approach thus represents a versatile and robust method to incorporate  $\Delta a Pro$  and OaPro residues into host

Finally, with mutated  $\beta$ -hairpin model peptides 12b and 13b in hand, we ascertained their ability to adopt native-like folds by NMR. The parent peptide of these analogues features a D-Pro-L-Pro type II'  $\beta$  turn and exhibits several key cross-strand NOE correlations in CDCl<sub>3</sub>.<sup>31</sup> The <sup>1</sup>H NMR spectrum of 12b in CDCl<sub>3</sub> revealed sharp, well-resolved peaks and the absence of any detectable minor amide rotamer signals. The J<sub>3</sub> NH-CH<sub>α</sub> coupling constants for Leu1, Val3, Leu6, and Val8 were large and ranged between 8.5 and 9.5 Hz, which is indicative of an extended conformation in the  $\beta$ -strand regions. The ROESY spectrum revealed several  $H\alpha_i$  to  $NH_{i+1}$  correlations that are also characteristic of extended conformations. A  $\beta$ -hairpin secondary structure for 12b was confirmed by cross-strand correlations between the H $\alpha$  protons of Phe2 and Phe7 and interstrand NH-NH correlations between Leu1 and Val8 as well as Val3 and Leu6 (Figure 8). Compound 13b was

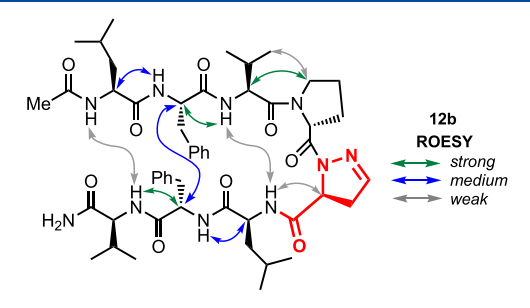


Figure 8. Interresidue Overhauser correlations indicating a  $\beta$ -hairpin structure in ΔaPro peptide 12b (600 MHz ROESY, CDCl<sub>3</sub>).

insoluble in CDCl<sub>3</sub>. Its <sup>1</sup>H NMR spectrum in DMSO- $d_6$  was complicated by the presence of rotameric signals and poor chemical shift dispersion, indicating a lack of the secondary structure. These results are consistent with our conformational analysis of monomers 4 and 6 and demonstrate that  $\Delta$ aPro is well-tolerated as a Pro surrogate within a  $\beta$ -turn.

## 3. DISCUSSION

Proline plays an important role in protein folding due to restricted backbone torsions, an appreciable population of its N-terminal *cis* amide rotamer, and its high *cis/trans* isomerization barrier relative to secondary amides. Several groups have investigated the factors leading to *trans* amide

stabilization in prolyl peptides. Extensive studies using γsubstituted prolines have led to a generally accepted model in which a stabilized  $C\gamma$  exo pyrrolidine pucker allows for optimal  $n \to \pi^*$  orbital overlap involving the N-acyl carbonyl donor and the C-terminal carbonyl acceptor—an interaction only possible in the *trans* amide conformation. Our investigation of aPro reveals a unique residue in which nearly isoenergetic endo and exo puckered forms are stabilized by  $n \rightarrow \sigma^*$  interactions within the pyrazolidine ring. Both puckered forms of aPro strongly favor the trans amide geometry ( $K_{trans/cis} = 12:1$  for 3 in D<sub>2</sub>O), which is wholly consistent with the trends observed for Piz and other N-heteroatom-substituted residues. The impact of the electronegative N $\delta$  on amide bond isomerization was clearly evident from Eyring analysis. The lower  $\Delta H^{\ddagger}$  value for 3 relative to Ac-Pro-OMe reflects a lower amide bond order and is largely responsible for its enhanced rate of isomerization. Taken together, these data show aPro to be a conformationally dynamic residue and suggests an ability to adopt the ring pucker or amide geometry that is contextually required by a host system.

Although a small number of aPro derivatives have been reported previously, we found that oxidation to the dihydropyrazole ( $\Delta a Pro$ ) ring occurred readily under ambient conditions. The rate of this reaction was slow enough in the case of 3 to allow for characterization of a pure sample. However, the rapid oxidation of peptides 11 indicates that aPro may have limited utility as a peptidomimetic residue. We thus urge caution in interpreting data from aPro-containing sequences given the customarily ample time between compound purification/characterization and biological or conformational experiments. In contrast, the  $\Delta a$ Pro residue is encountered in several biologically active peptidomimetics including AZD8165, a potent thrombin inhibitor that recently entered into phase I clinical trials. 15c Interestingly, the aPro analogue of AZD8165 was also identified as a potent cell permeable thrombin inhibitor but was not pursued further because of oxidative decomposition in vivo.

Conformational analysis of  $\Delta a$ Pro reveals a flat heterocycle analogous to that found in methanoprolines and dehydroprolines. We found the *trans* amide propensity of  $\Delta a$ Pro to be remarkably high because of coplanarity of the N $\delta$  lone pair electrons and the amide carbonyl oxygen. The calculated torsions for the unpuckered ring closely resemble those for Ac-Pro-OMe<sub>endo</sub>, albeit with a weaker  $n\rightarrow\pi^*$  interaction. This is likely a result of the electron-withdrawing effect of the sp<sup>2</sup> N $\delta$ and is reflected in the lower trans/cis isomerization barrier relative to Pro. The X-ray structure of 7 revealed an  $n\rightarrow\pi^*$ interaction with a Burgi-Dunitz trajectory and a donoracceptor distance similar to those observed in 4,5-methanoprolines.<sup>33</sup>  $\Delta$ aPro was also found to be well-tolerated within the type II'  $\beta$ -turn region of a model hairpin in place of L-Pro. Beyond its conformational impact, the hydrazone of  $\Delta a Pro$  can also be viewed as a chemically stable isostere of the enamine in  $\gamma$ , $\delta$ -dehydroproline. This residue was found to be important for the antimicrobial activity of the natural product promysalin but decomposes under mildly acidic conditions.<sup>34</sup> The synthetic approach to  $\Delta a Pro$  peptides described here should enable additional SAR studies on several biologically active peptidomimetics that harbor flattened proline surrogates.

The OaPro residue represents a novel building block that retains the planar heterocycle of  $\Delta a$ Pro but deviates considerably from both aPro and  $\Delta a$ Pro with respect to amide propensity. Conjugation of the N $\delta$  lone pair electrons

with the  $\gamma$  carbonyl group in OaPro results in conformational steering of the NH bond. The *trans* amide rotamer of Ac-OaPro-OMe (6) appears to suffer from a destabilizing 1,3-steric interaction that can be overcome by a stabilizing C5 H-bond with the amide oxygen in the *cis* rotamer. This interaction appears to be largely context dependent, as we observed a shift toward higher *trans* amide population in the case of peptide 13a ( $\sim$ 10:1). Here, the increased steric bulk of the Val side chain relative to the acetyl group in 6 likely destabilizes the *cis* conformer. As expected, OaPro exhibits the fastest rate of amide isomerization among the aPro variants due to strong induction from the  $\gamma$  carbonyl. This renders the backbone peptide bond of OaPro in structures such as 13 almost non-amide in character.

#### 4. CONCLUSIONS

In summary, we have demonstrated the stereoelectronic tuning of proline conformation through the introduction of heteroatomic functional groups at the  $\delta$  position. As part of this study, we report an electrophilic amination/late-stage cyclization approach that enables the synthesis of  $\Delta$ aPro and OaPro-containing peptides on solid support. Conformational analysis of aPro variants reveals residues in which lone pair repulsion and electron-withdrawing effects largely dictate heterocycle conformation and amide isomerization kinetics. These studies demonstrate the effective decoupling of ring puckering and  $n\rightarrow\pi^*$  stabilization effects from *trans/cis* amide propensities within a series of aPro oxidation state variants. The low rotational barriers of N-acyl aPro derivatives should enhance the rate of peptide backbone preorganization in cases where proyl amide isomerization is the rate-determining step. Coupled with divergent rotamer preferences, these qualities render  $\Delta a$ Pro and OaPro versatile conformational probes of protein folding and peptidomimetic substrate binding.

## 5. EXPERIMENTAL SECTION

**5.1. General Synthesis Notes.** Unless stated otherwise, reactions were performed in a flame-dried glassware under a positive pressure of argon or nitrogen gas using dry solvents. Commercial grade reagents and solvents were used without further purification except where noted. Anhydrous solvents were purchased directly from chemical suppliers. Thin-layer chromatography (TLC) was performed using silica gel 60 F254 precoated plates (0.25 mm). Flash chromatography was performed using silica gel (60  $\mu$ m particle size). Reaction progress was judged by TLC analysis (single spot/two solvent systems) using a UV lamp, CAM (ceric ammonium molybdate), ninhydrin, or basic KMnO<sub>4</sub> stain(s) for detection purposes. NMR spectra were recorded on a 400, 500, or 600 MHz spectrometer. Proton chemical shifts are reported as  $\delta$  values relative to residual signals from deuterated solvents (D<sub>2</sub>O, CDCl<sub>3</sub>, CD<sub>3</sub>OD, or DMSO- $d_6$ ).

**5.2.** Ac-(*N*-NHBoc)Hse(TBS)-OMe (2). To a solution of H-Hse(TBS)-OMe (1)<sup>24</sup> (1.08 g, 4.37 mmol) in a biphasic mixture of 25 mL THF and 25 mL sat aq NaHCO<sub>3</sub> was added 2-(*tert*-butyl) 3,3-diethyl 1,2-oxaziridine-2,3,3-tricarboxylate<sup>25</sup> (1.26 g, 4.37 mmol), and the reaction mixture was allowed to stir at rt for 2 h. The reaction was then quenched with 1 mL of ethylenediamine with stirring for an additional 5 min, diluted with EtOAc and the organic layer was washed with 1 M aq HCl and brine, dried over anhydrous Na<sub>2</sub>SO<sub>4</sub>, filtered, and concentrated. Purification by flash chromatography over silica gel (0–30% EtOAc/hexanes) afforded H-(*N*-NHBoc)Hse-(TBS)-OMe as a colorless oil (1.27 g, 80% yield). <sup>1</sup>H NMR (400 MHz, CDCl<sub>3</sub>): δ 6.29 (broad s, 1H), 3.81–3.67 (m, 6H), 2.00–1.78 (m, 2H), 1.43 (s, 9H), 0.87 (s, 9H), 0.04 (s, 6H); <sup>13</sup>C{<sup>1</sup>H} NMR (101 MHz, CDCl<sub>3</sub>): δ 173.8, 156.1, 80.4, 61.3, 60.1, 52.0, 33.3, 28.2,

28.1, 25.8, 18.2, -5.5; HRMS (ESI-TOF) m/z:  $[M + H]^+$  calcd for  $C_{16}H_{35}N_2O_5Si$ , 363.2301; found, 363.2318.

To a solution of H-(*N*-NHBoc)Hse(TBS)-OMe above (600 mg, 1.65 mmol) in 20 mL DCM was added NaHCO<sub>3</sub> (832 mg, 9.90 mmol) followed by dropwise addition of acetyl chloride (354  $\mu$ L, 4.96 mmol). The reaction mixture was allowed to stir at rt for 30 min, diluted with DCM, and washed with H<sub>2</sub>O and brine. The organic layer was dried over anhydrous Na<sub>2</sub>SO<sub>4</sub>, filtered, and concentrated. Purification by flash chromatography over silica gel (5–35% EtOAc/hexanes) afforded **2** as colorless oil (569 mg, 85% yield). <sup>1</sup>H NMR (400 MHz, CDCl<sub>3</sub>, mixture of rotamers):  $\delta$  7.09 (broad s, 1H), 5.42 (broad s, 1H), 3.84–3.61 (m, 5H), 2.13 (s, 3H), 2.09–2.00 (m, 1H), 1.86 (broad s, 1H), 1.52–1.42 (s, 9H), 0.89 (s, 9H), 0.10–0.00 (ss, 6H); <sup>13</sup>C{<sup>1</sup>H} NMR (101 MHz, CDCl<sub>3</sub>):  $\delta$  174.4, 172.9, 154.3, 81.5, 59.4, 54.8, 52.4, 31.7, 28.1, 25.8, 20.7, 18.2, –5.5; HRMS (ESI-TOF) m/z: [M + H]<sup>+</sup> calcd for C<sub>18</sub>H<sub>37</sub>N<sub>2</sub>O<sub>6</sub>Si, 405.2421; found, 405.2420.

**5.3.** Ac-aPro-OMe (3). To a solution of 2 (222 mg, 0.55 mmol) in 10 mL DCM was added  $Ph_3PCl_2$  (914 mg, 2.74 mmol). The reaction mixture was allowed to stir at rt for 30 min and concentrated. Purification of the crude residue by flash chromatography over silica gel (40–70% EtOAc/hexanes) afforded the primary alkyl chloride (102 mg, 60% yield), which was used immediately in the next step.

To a solution of the crude chloride (47 mg, 0.15 mmol) in 3 mL DMF was added K<sub>2</sub>CO<sub>3</sub> (105 mg, 0.76 mmol), and the reaction mixture was allowed to stir at 60 °C in an oil bath for 18 h. The reaction mixture was then concentrated, taken up in EtOAc, and washed with 1 M HCl and brine. The organic layer was dried over anhydrous Na<sub>2</sub>SO<sub>4</sub>, filtered, and concentrated. Purification by flash chromatography over silica gel (20-60% EtOAc/hexanes) afforded Ac-(N'-Boc)aPro-OMe as a colorless oil (33 mg, 80% yield). <sup>1</sup>H NMR (400 MHz, CDCl<sub>3</sub>, mixture of rotamers):  $\delta$  4.90 (dd, J = 8.4, 6.0 Hz, 0.9H), 4.37 (d, I = 9.2 Hz, 0.1 H), 4.27–4.05 (ddd, m, I =11.6, 8.8, 3.2 Hz, 0.9, 0.1 H), 3.78-3.63 (ss, 3H), 3.40-3.25 (m, 0.1H), 3.14-2.96 (m, 0.9H), 2.41-2.17 (m, 2H), 2.11 (s, 3H), 1.46 (s, 9H);  ${}^{13}C\{{}^{1}H\}$  NMR (101 MHz, CDCl<sub>3</sub>, mixture of rotamers):  $\delta$ 172.9, 171.0, 157.5, 156.8, 83.2, 82.5, 57.3, 56.6, 52.4, 47.8, 46.9, 31.2, 29.8, 28.0, 21.0, 20.6; HRMS (ESI-TOF) m/z:  $[M + Na]^+$  cacld for C<sub>12</sub>H<sub>20</sub>N<sub>2</sub>NaO<sub>5</sub>, 295.1264; found, 295.1266.

To a solution of Ac-(N'-Boc)aPro-OMe (167 mg, 0.61 mmol) was added 4 mL of a 90:5:5 mixture of TFA/DCM/TES, and the reaction mixture was allowed to stir at rt for 2 h. The reaction was then diluted with EtOAc, concentrated, taken up in DCM, and washed with sat aq NaHCO<sub>3</sub>. The aqueous layer was extracted with DCM, and the organic layers were combined, dried over anhydrous Na2SO4, filtered, and concentrated. Purification by flash chromatography over silica gel (0-7% MeOH/DCM) afforded 3 as a colorless oil (90 mg, 85% yield). <sup>1</sup>H NMR (400 MHz, CDCl<sub>3</sub>):  $\delta$  4.67 (dd, J = 9.2, 6.8 Hz, 1H), 3.72 (s, 3H), 3.23 (ddd, J = 11.2, 7.6, 2.4 Hz, 1H), 2.84 (ddd, 11.6, 9.6, 7.2 Hz, 1H), 2.56-2.44 (m, 1H), 2.17 (s, 3H), 2.09-1.95 (m, 1H); <sup>1</sup>H NMR (600 MHz, D<sub>2</sub>O, mixture of rotamers):  $\delta$  4.96–4.89 (m, 0.08 H), 4.58 (dd, J = 9, 6.6 Hz, 0.92H), 3.86 - 3.75 (s, 3H), 3.23(ddd, J = 12, 6.6, 5.4 Hz, 1H), 3.08-3.01 (m, 1H), 2.59 (dddd, J = 18, 11.4, 6.6, 5.4 Hz, 1H), 2.23-2.13 (m, 4H); <sup>13</sup>C{<sup>1</sup>H} NMR (101 MHz, CDCl<sub>3</sub>):  $\delta$  172.7, 171.1, 56.9, 52.4, 47.9, 33.4, 21.3; HRMS (ESI-TOF) m/z: [M + H]<sup>+</sup> calcd for C<sub>7</sub>H<sub>13</sub>N<sub>2</sub>O<sub>3</sub>, 173.0921; found,

**5.4. Ac-ΔaPro-OMe (4).** To a solution of 3 (24.0 mg, 0.14 mmol) in 5 mL DCM was added Et<sub>3</sub>N (195  $\mu$ L, 1.4 mmol) followed by I<sub>2</sub> (178 mg, 0.70 mmol) and the reaction mixture was allowed to stir at rt for 18 h. The reaction was then washed with 1 M aq Na<sub>2</sub>S<sub>2</sub>O<sub>3</sub>, 1 M aq HCl, and brine. The organic layer was dried over anhydrous Na<sub>2</sub>SO<sub>4</sub>, filtered, and concentrated. Purification by flash chromatography over silica gel (50–80% EtOAc/hexanes) afforded 4 as a colorless oil (19.0 mg, 80% yield) <sup>1</sup>H NMR (400 MHz, CDCl<sub>3</sub>): δ 6.86 (t, J = 1.6 Hz, 1H), 4.81 (dd, J = 12.4, 6.0 Hz, 1H), 3.76 (s, 3H), 3.24 (ddd, J = 18.8, 12.4, 1.6 Hz, 1H), 2.96 (ddd, 18.4, 6.0, 1.6 Hz, 1H), 2.34 (s, 3H); <sup>1</sup>H NMR (600 MHz, D<sub>2</sub>O): δ 7.26–7.24 (m, 1H), 4.91 (dd, J = 12, 5.4 Hz, 1H), 3.80 (s, 3H), 3.45 (m, 1H), 3.14 (m, 1H), 2.35 (s, 3H); <sup>13</sup>C{<sup>1</sup>H} NMR (151 MHz, CDCl<sub>3</sub>): δ 170.4,

169.2, 144.7, 55.4, 52.7, 38.7, 21.3; HRMS (ESI-TOF) m/z: [M + H]<sup>+</sup> calcd for  $C_7H_{11}N_7O_3$ , 171.0764; found, 171.0766.

**5.5.** Ac-OaPro-OMe (6). To a solution of  $5^{10b}$  (632 mg, 1.99 mmol) in 20 mL DCM was added NaHCO<sub>3</sub> (1.67 g, 19.9 mmol) followed by dropwise addition of acetyl chloride (425  $\mu$ L, 5.96 mmol), and the reaction mixture was allowed to stir at rt for 30 min. The reaction was then washed with H<sub>2</sub>O, brine, dried over anhydrous Na<sub>2</sub>SO<sub>4</sub>, filtered, and concentrated. Purification by flash chromatography over silica gel (10–40% EtOAc/hexanes) afforded Ac-(*N*-NHBoc)Asp(*t*Bu)-OMe as a white solid (526 mg, 73% yield).

To a solution of Ac-(N-NHBoc)Asp(tBu)-OMe above (50.0 mg, 0.139 mmol) in thionyl chloride (101  $\mu$ L, 1.39 mmol) was added H<sub>2</sub>O (0.005 mL, 0.278 mmol), and the reaction mixture was allowed to stir at rt for 3 h. The reaction was then diluted with DCM, dried over anhydrous K2CO3, filtered, and concentrated. Purification by flash chromatography over silica gel (0-4% MeOH/DCM) afforded 6 as a white solid (17 mg, 65% yield). <sup>1</sup>H NMR (600 MHz, CDCl<sub>3</sub>, mixture of rotamers):  $\delta$  5.26 (broad s, 0.3H), 4.89 (broad s, 0.6H), 3.82 (broad s, 3H), 3.33-3.05 (ss, 1H), 3.02-2.65 (ss, 1H), 2.28-1.94 (ss, 3H); <sup>1</sup>H NMR (600 MHz,  $D_2O_1$ , mixture of rotamers):  $\delta$ 5.38 (d, J = 11.4 Hz, 0.55H), 5.15 (d, J = 10.2 Hz, 0.45H), 3.89-3.79(ss, 3H), 3.45 (dd, J = 18, 11.4 Hz, 0.55H), 3.27 (dd, J = 18, 12 Hz, 0.45H), 3.02 (d, J = 18 Hz, 0.55H), 2.85 (d, J = 18 Hz, 0.45H), 2.20-2.07 (ss, 3H); 13C{1H} NMR (101 MHz, CDCl<sub>3</sub>, mixture of rotamers):  $\delta$  168.9, 166.6, 163.1, 56.8, 53.4, 35.4, 34.2, 20.8, 19.4; HRMS (ESI-TOF) m/z:  $[M + H]^+$  cacld for  $C_7H_{11}N_2O_4$ , 187.0713; found, 187,0709.

5.6. Synthesis of Ac-∆aPro-Gly-OBn (7). To a solution of H-HSer(TBS)-OH (1.0 g, 4.29 mmol) in a biphasic mixture of 40 mL THF and 40 mL sat aq NaHCO3 was added 2-(tert-butyl) 3,3-diethyl 1,2-oxaziridine-2,3,3-tricarboxylate<sup>25</sup> (1.24 g, 4.29 mmol), and the reaction mixture was allowed to stir at rt for 2 h. The reaction was then quenched with 1 mL of ethylenediamine with stirring for an additional 5 min, acidified to pH 3 with 1 M HCl, extracted with DCM, and the organic layer was dried over anhydrous Na2SO4. To the filtered organic layer was added H-Gly-OBn·HCl (2.6 g, 12.87 mmol), DIEA (4.48 mL, 25.7 mmol), HOBt·H<sub>2</sub>O (85 mg, 0.56 mmol), followed by EDC·HCl (905 mg, 4.72 mmol), and the reaction mixture was allowed to stir at rt for 18 h. The reaction was then washed with 1 M HCl, sat aq NaHCO3, brine, and the organic layer was dried over anhydrous Na2SO4, filtered, and concentrated. Purification by flash chromatography over silica gel (5-35% EtOAc/hexanes) afforded H-(N-NHBoc)HSer(TBS)-Gly-OBn as a colorless oil (1.04 g, 49% yield). <sup>1</sup>H NMR (400 MHz, CDCl<sub>3</sub>, mixture of rotamers):  $\delta$  8.27 (broad s, 1H), 7.42–7.28 (m, 5H), 6.79–6.58 (ss, 1H), 5.22-5.10 (ss, 2H), 4.22-3.98 (m, 2H), 3.90-3.62 (m, 3H), 2.11-1.77 (m, 1H), 1.54-1.35 (m, 10H), 0.89 (s, 9H), 0.11-0.05 (ss, 6H); 13C(1H) NMR (151 MHz, CDCl<sub>3</sub>, mixture of rotamers):  $\delta$  172.9, 172.5, 169.8, 169.7, 156.1, 135.2, 135.1, 128.6, 128.4, 128.3, 81.9, 81.1, 67.3, 67.1, 65.4, 64.9, 62.1, 60.8, 40.9, 32.9, 32.6, 28.2, 25.9, 25.6, 18.1, -3.6, -5.5; HRMS (ESI-TOF) m/z: [M +  $\label{eq:hamiltonian} H]^+ \ cald \ for \ C_{24} H_{42} N_3 O_6 Si, \ 496.2828; \ found, \ 496.2832.$ 

To a solution of H-(N-NHBoc)HSer(TBS)-Gly-OBn above (200 mg, 400  $\mu$ mol) in 10 mL DCM was added pyridine (196  $\mu$ L, 2.42 mmol) followed by dropwise addition of acetyl chloride (86  $\mu$ L, 1.21 mmol), and the reaction mixture was allowed to stir at rt for 1 h. The reaction was then washed with 1 M HCl, sat aq NaHCO $_3$ , brine, dried over anhydrous Na $_2$ SO $_4$ , filtered, and concentrated. Purification by flash chromatography over silica gel (30–40% EtOAc/hexanes) afforded Ac-(N-NHBoc)HSer(TBS)-Gly-OBn as colorless oil (174 mg, 81% yield), which was used directly in the following step.

To a solution of Ac-(N-NHBoc)HSer(TBS)-Gly-OBn (168 mg, 0.31 mmol) in 4.5 mL THF at 0 °C was added 1 M TBAF in THF (372  $\mu$ L, 0.37 mmol), and the reaction mixture was allowed to stir at rt for 1 h. The reaction was then acidified with 1 M HCl and extracted with EtOAc. The organic layer was washed with brine, dried over anhydrous Na<sub>2</sub>SO<sub>4</sub>, filtered, and concentrated. Purification by flash chromatography over silica gel (0–8% MeOH/DCM) afforded the primarily alcohol Ac-(N-NHBoc)HSer-Gly-OBn as colorless oil (107 mg, 82% yield). This oil was dissolved in 3 mL dry THF at -10 °C

and treated with a prestirred solution of PPh<sub>3</sub> (199 mg, 0.76 mmol) and DIAD (122  $\mu$ L, 0.58 mmol) in 3 mL dry THF at -10 °C in a dropwise fashion, and the reaction mixture was allowed to stir at rt for 1.5 h. The reaction was quenched with a few drops of H<sub>2</sub>O and concentrated. Purification by flash chromatography over silica gel (40–60% EtOAc/hexanes) afforded Ac-(N'-Boc)aPro-Gly-OBn as colorless oil (80 mg, 79% yield).

The resulting oil above was dissolved in 3 mL of 4 N HCl/dioxane, and the reaction mixture was allowed to stir for 1.5 h at rt. The reaction was then concentrated, taken up in EtOAc, washed with sat aq NaHCO<sub>3</sub>, brine, filtered, and concentrated. Purification by flash chromatography over silica gel (80–100% EtOAc/hexanes) afforded Ac-aPro-Gly-OBn as a white solid (24 mg, 40% yield). Attempts to crystalize the product from hexanes/DCM with heating using a heat gun afforded crystals of the oxidized compound 7 as a white crystalline solid. <sup>1</sup>H NMR (600 MHz, CDCl<sub>3</sub>):  $\delta$  7.96 (s, 1H), 7.39–7.32 (m, 5H), 6.97 (t, J = 1.7 Hz, 1H), 5.17 (s, 2H), 4.97 (dd, J = 12, 4.8 Hz, 1H), 4.06 (t, J = 4.8 Hz, 2H), 3.71 (ddd, J = 19.2, 4.8, 1.7 Hz, 1H), 3.00 (ddd, 19.2, 12, 1.7 Hz, 1H), 2.32 (s, 3H); <sup>13</sup>C NMR{<sup>1</sup>H} (151 MHz, CDCl<sub>3</sub>):  $\delta$  171.5, 169.1, 168.5, 148.9, 135.1, 128.0, 127.9, 127.8, 67.1, 56.5, 41.7, 36.2, 21.4; HRMS (ESI-TOF) m/z: [M + H] calcd for  $C_{15}H_{18}N_3O_4$ , 304.1292; found, 304.1307.

**5.7.** General Procedure for the Synthesis of Hydrazino Benzyl Esters (8). To a solution of either H-Hse(OTBS)-OBn or H-Asp(tBu)-OBn (1.0 equiv) in a 10:7 biphasic mixture of THF/sat. aq NaHCO<sub>3</sub> was added 2-(tert-butyl) 3,3-diethyl 1,2-oxaziridine-2,3,3-tricarboxylate<sup>25</sup> (1.0 equiv) in THF portionwise over 15 min. The reaction was allowed to stir at rt for 2.5 h, and then quenched with 1 mL ethylenediamine by stirring for an additional 5 min. The mixture was diluted with EtOAc, washed with H<sub>2</sub>O, and brine, and the organic layer was dried over anhydrous Na<sub>2</sub>SO<sub>4</sub>, filtered, and concentrated.

A solution of the appropriate Boc-protected hydrazino benzyl ester above (1.0 equiv) in DCM was treated with NaHCO $_3$  (10.0 equiv), followed by portionwise addition of either Fmoc-Val-Cl or Fmoc-(D)Pro-Cl (3.0 equiv) over 30 min. After 2 h, the reaction was washed with H $_2$ O, extracted with DCM, and the organic layer was dried over anhydrous Na $_2$ SO $_4$ , filtered, and concentrated.

- **5.8.** H-(*N*-NHBoc)Hse(OTBS)-OBn. Purification by flash chromatography over silica gel (10–20% EtOAc/hexanes) afforded H-(*N*-NHBoc)Hse(OTBS)-OBn as a colorless oil (7.69 g, 82% yield).  $^{1}$ H NMR (400 MHz, CDCl<sub>3</sub>):  $\delta$  7.37–7.27 (m, 5H), 6.37 (br s, 1H), 5.15 (d, J = 6.4 Hz, 2H), 4.11 (br s, 1H), 3.81 (dd, J = 7.6, 5.2 Hz, 1H), 3.77–3.67 (m, 1H), 2.07–1.73 (m, 2H), 1.42 (s, 9H), 0.86 (s, 9H), 0.02 (s, 6H);  $^{13}$ C{ $^{1}$ H} NMR (101 MHz, CDCl<sub>3</sub>):  $\delta$  173.3, 156.2, 135.6, 128.6, 128.3, 128.2, 80.4, 66.7, 61.3, 60.2, 33.4, 28.3, 25.9, 18.2, -5.4; HRMS (ESI-TOF) m/z: [M + H]<sup>+</sup> calcd for  $C_{22}H_{39}N_2O_5Si$ , 439.2628; found, 439.2620.
- **5.9.** H-(*N*-NHBoc)Asp(*t*Bu)-OBn. Purification by flash chromatography over silica gel (10–20% EtOAc/hexanes) afforded H-(*N*-NHBoc)Asp(*t*Bu)-OBn as an off-white solid (5.89 g, 74% yield).  $^1$ H NMR (400 MHz, CDCl<sub>3</sub>):  $\delta$  7.36–7.24 (m, 5H), 6.47 (br s, 1H), 5.15 (d, J = 12.5 Hz, 2H), 4.45 (br s, 1H):  $\delta$  3.89 (t, J = 5.6 Hz, 1H), 2.72 (d, J = 5.6 Hz, 2H), 1.41 (s, 9H), 1.37 (s, 9H);  $^{13}$ C{ $^1$ H} NMR (101 MHz, CDCl<sub>3</sub>):  $\delta$  172.0, 169.8, 156.3, 135.4, 128.6, 128.4, 128.3, 81.4, 80.6, 67.0, 59.6, 36.6, 28.3, 28.0; HRMS (ESI-TOF) m/z: [M + H] $^+$  calcd for C<sub>20</sub>H<sub>31</sub>N<sub>2</sub>O<sub>6</sub>, 395.2182; found, 395.2178.
- **5.10. Fmoc-Val-(***N***-NHBoc)Hse(TBS)-OBn (8a).** Purification by flash chromatography over silica gel (20% EtOAc/hexanes) gave a white solid (1.13 g, 65% yield).  $^1$ H NMR (400 MHz, CDCl<sub>3</sub>, mixture of rotamers):  $\delta$  7.78 (d, J = 7.5 Hz, 2H), 7.64 (d, J = 6.0 Hz, 2H), 7.54–7.19 (m, 9H), 5.60 (d, J = 8.7 Hz, 2H), 5.24–5.07 (m, 2H), 4.71 (br s, 1H), 4.47–4.18 (m, 3H), 3.91–3.64 (m, 2H), 2.30–1.81 (m, 3H), 1.62–1.42 (ss, 9H), 1.13–0.77 (m, 15H), 0.25 to (–)0.07 (m, 6H);  $^{13}$ C{ $^{1}$ H} NMR (101 MHz, CDCl<sub>3</sub>, mixture of rotamers):  $\delta$  175.0, 172.0, 171.0, 156.1, 156.0, 154.2, 143.9, 141.3, 135.0, 128.7, 128.5, 128.3, 127.6, 127.1, 125.2, 119.9, 81.8, 82.3, 67.4, 66.9, 59.2, 55.8, 53.5, 47.2, 31.4, 28.1, 25.9, 19.8, 18.2, 16.7, –5.4, –5.5; HRMS (ESI-TOF) m/z: [M + H] $^+$  calcd for C $_{42}$ H $_{58}$ N $_3$ O $_8$ Si, 760.3993; found, 760.3998.

- **5.11. Fmoc-(D)Pro-(***N***-NHBoc)Hse(TBS)-OBn (8b).** Purification by flash chromatography over silica gel (20–30% EtOAc/hexanes) gave a white solid (1.72 g, 77% yield).  $^{1}$ H NMR (400 MHz, CDCl<sub>3</sub>, mixture of rotamers):  $\delta$  7.77 (d, J = 7.5 Hz, 2H), 7.67–7.53 (m, 2H), 7.48–7.08 (m, 9H), 5.58–5.27 (m, 1H), 5.17 (q, J = 11.6 Hz, 2H), 5.0–4.60 (m, 2H), 4.40–4.16 (m, 3H), 3.85–3.66 (m, 3H), 3.61–3.48 (m, 1H), 2.30–1.77 (m, 6H), 1.56–1.44 (ss, 9H), 0.89 (s, 9H), 0.12 to (–)0.02 (m, 6H);  $^{13}$ C{ $^{1}$ H} NMR (101 MHz, CDCl<sub>3</sub>, mixture of rotamers):  $\delta$  176.5, 176.2, 171.0, 154.8, 154.6, 154.1, 144.5, 144.1, 143.9, 141.3, 135.5, 135.0, 128.4, 128.1, 128.0, 127.6, 127.0, 125.2, 119.9, 81.6, 67.5, 67.0, 59.3, 56.3, 55.6, 47.2, 31.8, 31.7, 31.0, 29.9, 28.1, 25.9, 24.5, 23.4, 18.2, –3.6, –5.4; HRMS (ESI-TOF) m/z: [M + H] $^{+}$  calcd for C<sub>42</sub>H<sub>56</sub>N<sub>3</sub>O<sub>8</sub>Si, 758.3836; found, 758.3831.
- **5.12. Fmoc-Val-(***N***-NHBoc)Asp(tBu)-OBn (8c).** Purification by flash chromatography over silica gel (10–30% EtOAc/hexanes) gave a white solid (1.76 g, 97% yield). <sup>1</sup>H NMR (400 MHz, CDCl<sub>3</sub>, mixture of rotamers):  $\delta$  7.76 (d, J = 7.5 Hz, 2H), 7.69–7.52 (m, 2H), 7.48–7.21 (m, 9.5H), 6.84 (br s, 0.5H), 5.86–5.26 (m, 1H), 5.25–5.04 (m, 2H), 4.77–4.48 (m, 1H), 4.45–4.13 (m, 3H), 3.25 (br s, 0.5H), 3.05–2.63 (m, 1.5H), 2.16–1.99 (m, 1H), 1.59–1.33 (ss, 18H), 1.8–0.80 (m, 6H);  $^{13}$ C{ $^{14}$ H} NMR (101 MHz, CDCl<sub>3</sub>, mixture of rotamers):  $\delta$  174.4, 169.7, 169.3, 156.0, 154.0, 143.8, 141.2, 134.9, 128.6, 128.4, 128.3, 127.6, 127.0, 125.2, 119.9, 82.9, 81.7, 67.7, 66.9, 55.6, 55.1, 47.2, 34.8, 31.4, 30.0, 28.1, 19.7, 17.4, 16.7; HRMS (ESITOF) m/z: [M + Na]<sup>+</sup> cacld for C<sub>40</sub>H<sub>49</sub>N<sub>3</sub>NaO<sub>9</sub>, 738.3366; found, 738.3360.
- **5.13. Fmoc-(D)Pro-(N-NHBoc)Asp(tBu)-OBn (8d).** Purification by flash chromatography over silica gel (20–40% EtOAc/hexanes) gave a white solid (1.40 g, 77% yield).  $^{1}$ H NMR (400 MHz, CDCl<sub>3</sub>, mixture of rotamers):  $\delta$  7.77 (d, 7.5 Hz, 2H), 7.67–7.55 (m, 2H), 7.46–7.09 (m, 8.5H), 6.91 (br s, 0.5H), 5.78–5.41 (m, 1H), 5.17 (s, 2H), 4.92–4.72 (m, 2H), 4.49–4.18 (m, 3H), 3.78–3.64 (m, 1H), 3.61–3.47 (m, 1H), 2.97–2.74 (m, 2H), 2.65–1.77 (m, 4H), 1.56–1.34 (m, 18H);  $^{13}$ C{ $^{1}$ H} NMR (101 MHz, CDCl<sub>3</sub>, mixture of rotamers):  $\delta$  175.7, 175.3, 169.4, 169.2, 168.9, 154.9, 154.8, 154.5, 154.2, 144.4, 143.9, 141.3, 135.3, 134.9, 128.5, 128.2, 127.7, 127.6, 127.1, 127.0, 125.3, 125.2, 120.0, 82.3, 81.8, 81.4, 81.2, 67.6, 67.4, 56.1, 55.8, 47.2, 46.8, 35.1, 30.7, 29.7, 28.2, 28.0, 24.6, 23.5; HRMS (ESI-TOF) m/z: [M + H] $^{+}$  calcd for C<sub>40</sub>H<sub>48</sub>N<sub>3</sub>O<sub>9</sub>, 714.3390; found, 714.3386.
- **5.14.** General Hydrogenolysis Procedure for the Synthesis of *N*-Amino Dipeptide Acids (9). A solution of ester 8 (1.0 equiv) in EtOAc was treated with 10% Pd/C (0.2 g/mmol of substrate) and stirred under  $\rm H_2$  atmosphere at rt until the starting material was consumed (3–4 h as indicated by TLC). The reaction mixture was filtered through Celite and concentrated.
- **5.15. Fmoc-Val-(N-NHBoc)Hse(TBS)-OH (9a).** Purification by flash chromatography over silica gel (10–40% EtOAc/hexanes) gave a white solid (650 mg, 65% yield). <sup>1</sup>H NMR (400 MHz, CDCl<sub>3</sub>, mixture of rotamers):  $\delta$  8.60–8.44 (m, 0.5H), 8.14 (s, 0.5H), 7.76 (d, J = 7.2 Hz, 2H), 7.68–7.54 (m, 2H), 7.47–7.24 (m, 4H), 5.88–5.48 (m, 1H), 4.96–4.12 (m, 5H), 4.01–3.60 (m, 2H), 2.36–1.78 (m, 3H), 1.63–1.23 (m, 9H) 1.17–0.69 (m, 15H), 0.35 to (–)0.17 (m, 6H);  $^{13}$ C{ $^{1}$ H} NMR (101 MHz, CDCl<sub>3</sub>):  $\delta$  175.2, 173.6, 171.9, 171.6, 156.7, 156.0, 143.9, 143.7, 141.2, 127.6, 127.1, 125.2, 119.9, 84.6, 84.4, 83.7, 67.4, 67.0, 61.4, 60.3, 59.6, 55.6, 47.2, 31.2, 30.9, 28.0, 27.7, 25.9, 25.6, 19.7, 18.2, 16.9, –3.7, –5.5; HRMS (ESI-TOF) m/z: [M + Na]<sup>+</sup> calcd for C<sub>35</sub>H<sub>51</sub>N<sub>3</sub>NaO<sub>8</sub>Si, 692.3343; found, 692.3340.
- **5.16. Fmoc-(D)Pro-(***N***-NHBoc)Hse(TBS)-OH (9b).** Purification by flash chromatography over silica gel (40–80% EtOAc/hexanes) gave a white solid (926 mg, 68% yield). <sup>1</sup>H NMR (400 MHz, CDCl<sub>3</sub>, mixture of rotamers):  $\delta$  8.58 (s, 0.25H), 8.18 (s, 0.5H), 7.75 (d, J = 7.4 Hz, 2H), 7.57 (dd, J = 10.5, 7.5 Hz, 2H), 7.39 (t, J = 7.5 Hz, 2H), 7.34–7.25 (m, 2H), 7.11 (s, 0.25H), 4.94–4.65 (m, 1H), 4.60–4.07 (m, 4H), 3.92–3.44 (m, 4H), 2.48–1.79 (m, 6H), 1.57–1.42 (m, 9H) 0.95–0.83 (m, 9H), 0.16 to (–)0.10 (m, 6H);  $^{13}$ C{ $^{1}$ H} NMR (101 MHz, CDCl<sub>3</sub>):  $\delta$  174.2, 170.2, 157.2, 155.0, 143.9, 143.7, 141.2, 127.7, 127.0, 125.1, 119.9, 83.9, 67.9, 67.7, 59.3, 56.2, 56.0, 47.1, 46.7, 30.9, 30.7, 29.1, 29.0, 28.1, 25.9, 25.6, 24.5, 18.1, 18.0, –3.6, –5.4;

- HRMS (ESI-TOF) m/z: [M + H]<sup>+</sup> calcd for  $C_{35}H_{50}N_3O_8Si$ , 668.3367; found, 668.3362.
- **5.17. Fmoc-Val-(***N***-NHBoc)Asp(tBu)-OH (9c).** Purification by flash chromatography over silica gel (40–80% EtOAc/hexanes) gave a white solid (810 mg, 60% yield). <sup>1</sup>H NMR (400 MHz, CDCl<sub>3</sub>, mixture of rotamers):  $\delta$  7.79–7.69 (m, 3H), 7.61–7.54 (m, 2H), 7.46–7.28 (m, 4H), 5.39 (d, J = 9.5 Hz, 1H), 4.65 (dd, J = 9.5, 6.3 Hz, 1H), 4.39–4.27 (m, 2H), 4.25–4.17 (m, 1H), 4.10–3.96 (m, 1H), 3.29 (dd, J = 19.1, 11.2 Hz, 1H), 3.19–3.08 (m, 1H), 2.04–1.87 (m, 1H), 1.60–1.18 (m, 18H), 1.05–0.76 (m, 6H); <sup>13</sup>C{<sup>1</sup>H} NMR (101 MHz, CDCl<sub>3</sub>, mixture of rotamers):  $\delta$  173.7, 172.4, 167.5, 158.3, 156.0, 143.9, 143.8, 141.3, 141.2, 127.7, 127.2, 127.1, 125.2, 125.2, 120.0, 119.9, 100.0, 85.9, 82.2, 67.1, 63.6, 60.4, 54.9, 47.1, 34.2, 31.4, 28.1, 28.0, 19.3, 17.3, 14.2; HRMS (ESI-TOF) m/z: [M + H]<sup>+</sup> calcd for C<sub>33</sub>H<sub>44</sub>N<sub>3</sub>O<sub>9</sub>, 626.3072; found, 626.3072.
- **5.18.** Fmoc-(D)Pro-(*N*-NHBoc)Asp(*t*Bu)-OH (9d). Purification by flash chromatography over silica gel (40–70% EtOAc/hexanes) gave a white solid (695 mg, 81% yield).  $^1$ H NMR (400 MHz, CDCl<sub>3</sub>, mixture of rotamers): δ 8.34 (s, 1H) 7.82–7.71 (m, 2H), 7.63–7.50 (m, 2H), 7.40 (t, J = 7.5 Hz, 2H), 7.36–7.28 (m, 2H), 4.72 (t, J = 5.7 Hz, 0.75H), 4.65–4.50 (m, 0.25H), 4.40–4.07 (m, 3H), 3.71–3.61 (m, 1H), 3.59–3.45 (m, 1H), 3.20–2.96 (m, 2H), 2.29–2.10 (m, 1H), 2.07–1.85 (m, 3H), 1.63–1.37 (m, 17H), 1.16 (s, 1H);  $^{13}$ C{ $^1$ H} NMR (101 MHz, CDCl<sub>3</sub>, mixture of rotamers): δ 174.0, 171.2, 168.5, 157.7, 154.9, 143.9, 143.7, 141.2, 127.7, 127.0, 125.1, 125.0, 119.9, 84.4, 81.5, 67.6, 62.5, 55.9, 47.1, 46.7, 34.5, 28.9, 28.0, 24.5; HRMS (ESI-TOF) m/z: [M + H] $^+$  calcd for C<sub>33</sub>H<sub>42</sub>N<sub>3</sub>O<sub>9</sub>, 624.2921; found, 624.2901.
- 5.19. Solid-Phase Synthesis of Peptides 12 and 13. Solidphase peptide synthesis was carried out on the Fmoc-capped polystyrene rink amide MBHA resin (100-200 mesh, 0.05-0.10 mmol scale). The following amino acid derivatives suitable for Fmoc SPPS were used: Boc-Ala-OH, Fmoc-Phe-OH, Fmoc-Val-OH, Fmoc-Leu-OH, and Fmoc-Ile-OH. Dry resin was washed with DMF 3× and allowed to swell in DMF for 30 min, and then treated with a solution of 20% piperidine/DMF (15 min × 2) and washed with DMF 3× prior to use. All reactions were carried out with gentle agitation. Fmoc deprotection steps were carried out by treating the resin with a solution of 20% piperidine/DMF (15 min × 2). Coupling of Fmocprotected amino acids was effected using 5 equiv. HATU (0.25-0.50 M in DMF), 10 equiv NMM (0.25-0.50 M in DMF), and 5 equiv of the carboxylic acid in DMF at 50 °C (microwave heating, 1 h). After each reaction the resin was washed with DMF 2x, DCM 1x, then DMF 1x. N-terminal acetylation for peptides 12b and 13b was effected using 25 equiv acetic anhydride (2.5 M in DCM) and 50 equiv pyridine (5.0 M in DCM) 2x. Peptides were cleaved from the resin by incubating with gentle stirring in 3 mL of 90:5:5 TFA/TES/ DCM at rt for 1 h. These conditions promoted concomitant cyclization of aAsp to form OaPro residues. The cleavage mixture was filtered, and the resin was rinsed with an additional 2 mL of cleavage solution. The filtrate was treated with 40 mL of cold Et<sub>2</sub>O to induce precipitation. The mixture was centrifuged, and the supernatant was removed. The remaining solid was washed 2 more times with Et<sub>2</sub>O and dried under vacuum. Peptides were analyzed and purified on C12 RP-HPLC columns (preparative: 4  $\mu$ , 90 Å, 250  $\times$  21.2 mm; analytical: 4  $\mu$ , 90 Å, 150 × 4.6 mm) using linear gradients of H<sub>2</sub>O/ MeCN (with 0.1% formic acid), and then lyophilized to afford white powder. All peptides were characterized by LCMS (ESI), HRMS (ESI-TOF), and <sup>1</sup>H NMR. Analytical HPLC samples for all purified peptides were acquired with linear gradients of MeCN in H<sub>2</sub>O (0.1% formic acid) over 20 min and spectra are provided for  $\lambda = 254$  nm.

Peptides harboring aPro (and ΔaPro) residues were prepared via on-resin silyl deprotection and Mitsunobu cyclization prior to cleavage. Peptides **12a** and **13a** were terminated with Boc-protected amino acids in order to protect against undesired Fmoc cleavage during these steps. Resin-bound HSer-containing peptides were thus treated with 1 M TBAF in THF for 6 h at rt. After the reaction, the resin was washed with THF 3×, DCM 3×, sat. aq NH<sub>4</sub>Cl 5×, H<sub>2</sub>O 5×, DCM 3×, and THF 3×. The resin was then treated with 5 equiv PPh<sub>3</sub> in THF followed by 5 equiv of DIAD, stirred for 12 h rt, this

reaction was repeated, and the resin was washed with THF 3× and DCM 3x. Peptides were subjected to cleavage, precipitation, and purification as described above. Analysis of crude cleavage mixtures revealed significant amounts (10-50%) of oxidized  $\Delta a Pro$  peptides in addition to aPro analogues. Attempted isolation of aPro peptides and analysis by HPLC revealed air oxidation to be sufficiently rapid so as to preclude characterization of analytically pure samples. Peptides harboring  $\Delta a Pro$  were readily isolated in pure form by preparative RP-HPLC.

5.20. Synthesis of 12b via Oxidation with H<sub>2</sub>O<sub>2</sub>. A portion of crude 11b was dissolved in 50% MeCN/H2O solution and treated with an equal volume of aq 30% H<sub>2</sub>O<sub>2</sub>. The reaction was carried out with gentle agitation. The oxidation rate was monitored via HPLC and complete after 24 h. The mixture was diluted with H<sub>2</sub>O and then concentrated to remove MeCN. The resulting solution was frozen and lyophilized to afford a crude powder. The crude powder was purified as described above.

**5.21.** H-Ala-Val-ΔaPro-Ile-NH<sub>2</sub>·HCOOH (12a). Obtained as a white powder (4 mg, 10% yield). <sup>1</sup>H NMR (400 MHz,  $D_2O$ ):  $\delta$  8.46 (s, 1H) 7.27 (s, 1H), 5.00 (d, I = 6.5 Hz, 1H), 4.23–4.05 (m, 2H), 3.42 (dd, J = 19.5, 12.5 Hz, 1H), 3.00 (dd, J = 19.5, 5.5 Hz, 1H),2.33-2.16 (m, 1H), 1.97-1.80 (m, 1H), 1.64-1.41 (m, 4H), 1.36-1.17 (m, 1H), 1.11–0.82 (m, 12H); HRMS (ESI-TOF) m/z: [M + H]<sup>+</sup> calcd for C<sub>18</sub>H<sub>33</sub>N<sub>6</sub>O<sub>4</sub>, 397.2558; found, 397.2565.

5.22. Ac-Leu-Phe-Val-pro-ΔaPro-Leu-Phe-Val-NH<sub>2</sub> (12b). Obtained as a white powder (5 mg, 6% yield). <sup>1</sup>H NMR (600 MHz, CDCl<sub>3</sub>):  $\delta$  8.80 (d, J = 9.5 Hz, 1H), 7.99 (d, J = 8.3 Hz, 1H), 7.91 (d, J = 9.7 Hz, 1H), 7.29–7.23 (m, 5H), 7.18–7.10 (m, 2H), 7.08-7.04 (m, 1H), 7.03-6.97 (m, 4H), 6.61 (d, J = 7.5 Hz, 2H), 6.28 (d, J = 8.3 Hz, 1H), 5.46 - 5.36 (m, 3H), 4.97 (dd, J = 13, 4.2 Hz, 1.2 Hz, 1.21H), 4.63-4.52 (m, 3H), 4.48 (q, J = 7.5 Hz, 1H), 4.20 (dd, J = 9.7, 6.8 Hz, 1H), 3.89-3.72 (m, 2H), 3.51 (d, J = 13.5 Hz, 1H), 3.35 (dd, I = 19, 13 Hz, 1H), 3.17 (dd, I = 19, 3.3 Hz, 1H), 2.91–2.77 (m, 3H), 2.25-2.16 (m, 2H), 2.13-2.05 (m, 2H), 2.04-1.93 (m, 4H), 1.89-1.80 (m, 1H), 1.71-1.62 (m, 1H), 1.57-1.47 (m, 2H), 1.46-1.39 (m, 1H), 1.38-1.31 (m, 1H), 0.98-0.76 (m, 21H), 0.64 (d, J = 6.5Hz, 3H); HRMS (ESI-TOF) m/z:  $[M + H]^+$  calcd for  $C_{51}H_{75}N_{10}O_{9}$ , 971.5713; found, 971.5718.

5.23. H-Ala-Val-OaPro-Ile-NH2:HCOOH (13a). Obtained as a white powder (17.6 mg, 43% yield). <sup>1</sup>H NMR (400 MHz, D<sub>2</sub>O, mixture of rotamers):  $\delta$  8.40 (s, 1H), 5.45–5.35 (m, 0.09H), 4.92 (dd, J = 11.3, 5.4 Hz, 0.91H), 4.72 (d, J = 6.9 Hz, 1H), 4.23-3.99 (m, J = 6.9 Hz, 1H), 4.22H), 3.55–3.35 (m, 0.09H), 3.06 (dd, *J* = 17.2, 11.3 Hz, 0.91H), 2.86 (dd, J = 15.8, 6.8 Hz, 0.09H), 2.60 (dd, J = 17.2, 5.4 Hz, 0.91H), 2.25-1.98 (m, 1H), 1.91-1.72 (m, 1H), 1.58-1.41 (m, 4H), 1.30-1.11 (m, 1H), 1.05–0.78 (m, 12H); HRMS (ESI-TOF) m/z: [M + H]<sup>+</sup> calcd for  $C_{18}H_{33}N_6O_5$ , 413.2507; found, 413.2510.

5.24. Ac-Leu-Phe-Val-pro-OaPro-Leu-Phe-Val-NH<sub>2</sub> (13b). Obtained as a white powder (42 mg, 46% yield). <sup>1</sup>H NMR (600 MHz, DMSO, mixture of rotamers):  $\delta$  8.65–8.45 (m, 1H), 8.31–8.12 (m, 2H), 8.08-7.65 (m, 4H), 7.30-6.99 (m, 9H), 6.88-6.75 (m, 2H), 5.41-5.29 (m, 0.5H), 5.03-4.93 (m, 1H), 4.82-4.68 (m, 0.5H), 4.60-4.29 (m, 4H), 4.27-3.96 (m, 2.5H), 3.65-3.51 (m, 1.5H), 3.25-2.58 (m, 5H), 2.47-2.27 (m, 0.5H), 2.12-1.70 (m, 6.5H), 1.64-1.16 (m, 8H), 0.93-0.56 (m, 24H); HRMS (ESI-TOF) m/z: [M + H]<sup>+</sup> calcd for C<sub>51</sub>H<sub>75</sub>N<sub>10</sub>O<sub>10</sub>, 987.5662; found, 987.5662.

5.25. Synthesis of Fmoc-Gly-(N-NHBoc)Hse-((R)- $\alpha$ -methyl)benzylamide. To a solution of H-(N-NHBoc)Hse-OBn (223 mg, 0.51 mmol) in 10 mL DCM was added NaHCO3 (428 mg, 5.10 mmol) followed by portion wise addition of Fmoc-Gly-Cl, and the reaction mixture was allowed to stir at rt for 2 h. The reaction was then diluted with more DCM, washed with H2O and brine, dried over anhydrous Na2SO4, filtered, and concentrated. Purification by flash chromatography over silica gel (10-30% EtOAc/hexanes) afforded the Fmoc-protected dipeptide benzyl ester as a white solid (290 mg, 79% yield).

To a solution of the dipeptide above (280 mg, 0.39 mmol) in 10 mL EtOAc was added 10% Pd/C (78 mg, 0.073 mmol), and the reaction mixture was allowed to stir under a H2 atmosphere at rt for 2.5 h. The reaction was then filtered through Celite and concentrated.

Purification by flash chromatography over silica gel (10-50% EtOAc/ hexanes) afforded the Fmoc-protected dipeptide free acid as a white solid (195 mg, 80% yield).

To a solution of the dipeptide free acid (92 mg, 0.147 mmol) in 5 mL DMF at 50 °C (using a heating mantle) was added N-methyl morpholine (48  $\mu$ L, 0.44 mmol), (R)- $\alpha$ -methylbenzylamine (28  $\mu$ L, 0.22 mmol), followed by HCTU (73 mg, 0.18 mmol), and the reaction mixture was allowed to stir at 50 °C for 2.5 h. The reaction was then concentrated and reconstituted in 20 mL EtOAc to which 20 mL 1 M aq HCl was added, and the biphasic mixture was stirred vigorously for 20 min to ensure deprotection of the silyl ether. The organic layer was then separated, washed with brine, dried over anhydrous Na<sub>2</sub>SO<sub>4</sub>, filtered, and concentrated. Purification by flash chromatography over silica gel (70-100% EtOAc/hexanes) afforded the final product as a colorless oil (24 mg, 26% yield). <sup>1</sup>H NMR (400 MHz, CDCl<sub>3</sub>, mixture of rotamers):  $\delta$  8.51 (d, J = 7.6 Hz, 1H), 8.01 (s, 1H), 7.84-7.69 (m, 3H), 7.59 (d, J = 7.6 Hz, 2H), 7.45-7.35 (m, 2H), 7.33-7.13 (m, 6H), 5.70-5.55 (m, 1H), 5.15-4.92 (m, 2H), 4.40-4.28 (m, 3H), 4.27-4.17 (m, 1H), 3.94-3.54 (m, 3H), 3.15 (s, 1H), 2.30-2.17 (m, 1H), 2.16-2.04 (m, 1H), 2.03-1.90 (m, 1H), 1.53-1.37 (m, 12H); <sup>13</sup>C{<sup>1</sup>H} NMR (101 MHz, CDCl<sub>3</sub>, mixture of rotamers):  $\delta$  173.5, 169.9, 156.9, 156.3, 155.9, 143.8, 143.7, 143.6, 141.3, 128.4, 127.7, 127.1, 126.1, 125.2, 120.0, 83.4, 83.0, 67.4, 67.2, 61.6, 60.8, 49.5, 47.0, 42.5, 29.6, 28.2, 28.1, 22.5, 22.2; HRMS (ESI-TOF) m/z:  $[M + H]^+$  calcd for  $C_{34}H_{41}N_4O_7$ , 617.2970; found, 617.2970.

#### ASSOCIATED CONTENT

#### Supporting Information

The Supporting Information is available free of charge at https://pubs.acs.org/doi/10.1021/acs.joc.9b03384.

NMR spectra, HPLC traces, NMR assignments and ROESY spectrum,1D NOESY spectra, 2D NOESY spectra, determination of cis/trans rate constants, diastereopurity determination for dipeptide fragment coupling, X-ray diffraction data, oxidation of 11b with  $H_2O_2$ , and computational studies (PDF)

(CIF)

(CIF)

#### AUTHOR INFORMATION

## **Corresponding Author**

Juan R. Del Valle – Department of Chemistry & Biochemistry, University of Notre Dame, Notre Dame, Indiana 46556, United States; o orcid.org/0000-0002-7964-8402; Email: jdelvalle@nd.edu

## **Authors**

Yassin M. Elbatrawi – Department of Chemistry & Biochemistry, University of Notre Dame, Notre Dame, Indiana 46556, United States

**Kyle P. Pedretty** – Department of Chemistry, University of South Florida, Tampa, Florida 33620, United States

Nicole Giddings – Department of Chemistry, University of South Florida, Tampa, Florida 33620, United States

H. Lee Woodcock - Department of Chemistry, University of South Florida, Tampa, Florida 33620, United States; orcid.org/0000-0003-3539-273X

Complete contact information is available at: https://pubs.acs.org/10.1021/acs.joc.9b03384

#### **Notes**

The authors declare no competing financial interest.

## ACKNOWLEDGMENTS

We gratefully acknowledge Dr. Lukasz Wojtas for carrying out X-ray diffraction studies, and Dr. Edwin Rivera (USF Interdisciplinary NMR Facility) and Dr.Evgenii Kovrigin (Notre Dame Magnetic Resonance Research Center) for assistance with NMR acquisitions. This work was supported by a grant from the National Science Foundation (CHE1709927).

#### REFERENCES

- (1) (a) Stewart, D. E.; Sarkar, A.; Wampler, J. E. Occurrence and role ofcis peptide bonds in protein structures. *J. Mol. Biol.* **1990**, 214, 253–260. (b) MacArthur, M. W.; Thornton, J. M. Influence of proline residues on protein conformation. *J. Mol. Biol.* **1991**, 218, 397–412. (c) Weiss, M. S.; Jabs, A.; Hilgenfeld, R. Peptide bonds revisited. *Nat. Struct. Mol. Biol.* **1998**, 5, 676. (d) Jabs, A.; Weiss, M. S.; Hilgenfeld, R. Non-proline Cis peptide bonds in proteins 11Edited by R. Huber. *J. Mol. Biol.* **1999**, 286, 291–304.
- (2) For selected examples, see the following and references cited therein: (a) Brandts, J. F.; Halvorson, H. R.; Brennan, M. Consideration of the Possibility That the Slow Step in Protein Denaturation Reactions is Due to Cis-Trans Isomerism of Proline Residues. *Biochemistry* 1975, 14, 4953–4963. (b) Wedemeyer, W. J.; Welker, E.; Scheraga, H. A. Proline Cis-Trans Isomerization and Protein Folding. *Biochemistry* 2002, 41, 14637–14644. (c) Lu, K. P.; Finn, G.; Lee, T. H.; Nicholson, L. K. Prolyl cis-trans isomerization as a molecular timer. *Nat. Chem. Biol.* 2007, 3, 619–629. (d) Shoulders, M. D.; Raines, R. T. Collagen Structure and Stability. *Annu. Rev. Biochem.* 2009, 78, 929–958.
- (3) (a) Torbeev, V. Y.; Hilvert, D. Both the equilibrium and isomerization dynamics of a single proline amide modulate  $\beta$ 2microglobulin amyloid assembly. Proc. Natl. Acad. Sci. U.S.A. 2013, 110, 20051. (b) Lummis, S. C. R.; Beene, D. L.; Lee, L. W.; Lester, H. A.; Broadhurst, R. W.; Dougherty, D. A. Cis-trans isomerization at a proline opens the pore of a neurotransmitter-gated ion channel. Nature 2005, 438, 248-252. (c) Lukesch, M. S.; Pavkov-Keller, T.; Gruber, K.; Zangger, K.; Wiltschi, B. Substituting the catalytic proline of 4-oxalocrotonate tautomerase with non-canonical analogues reveals a finely tuned catalytic system. Sci. Rep. 2019, 9, 2697. (d) Holzberger, B.; Marx, A. Replacing 32 Proline Residues by a Noncanonical Amino Acid Results in a Highly Active DNA Polymerase. J. Am. Chem. Soc. 2010, 132, 15708-15713. (e) Golbik, R.; Yu, C.; Weyher-Stingl, E.; Huber, R.; Moroder, L.; Budisa, N.; Schiene-Fischer, C. Peptidyl Prolyl cis/trans-Isomerases: Comparative Reactivities of Cyclophilins, FK506-Binding Proteins, and Parvulins with Fluorinated Oligopeptide and Protein Substrates. Biochemistry 2005, 44, 16026-16034.
- (4) For reviews on the gauche effect in  $\gamma$ -substituted prolines see: (a) Horng, J.-C.; Raines, R. T. Stereoelectronic effects on polyproline conformation. *Protein Sci.* **2006**, *15*, 74–83. (b) Hinderaker, M. P.; Raines, R. T. An electronic effect on protein structure. *Protein Sci.* **2003**, *12*, 1188–1194.
- (5) (a) Milner-White, E. J.; Bell, L. H.; Maccallum, P. H. Pyrrolidine ring puckering in cis and trans-proline residues in proteins and polypeptides: Different puckers are favoured in certain situations. *J. Mol. Biol.* **1992**, 228, 725–734. (b) Vitagliano, L.; Berisio, R.; Mastrangelo, A.; Mazzarella, L.; Zagari, A. Preferred proline puckerings in cis and trans peptide groups: implications for collagen stability. *Protein sci.* **2001**, *10*, 2627–32. (c) Madison, V. Flexibility of the pyrrolidine ring in proline peptides. *Biopolymers* **1977**, *16*, 2671–2692. (d) Newberry, R. W.; Raines, R. T. The  $n \rightarrow \pi^*$  Interaction. *Acc. Chem. Res.* **2017**, *50*, 1838–1846. (e) Bartlett, G. J.; Choudhary, A.; Raines, R. T.; Woolfson, D. N.  $n \rightarrow \pi^*$  interactions in proteins. *Nat. Chem. Biol.* **2010**, *6*, 615–620.
- (6) (a) Kern, D.; Schutkowski, M.; Drakenberg, T. Rotational Barriers of cis/trans Isomerization of Proline Analogues and Their Catalysis by Cyclophilin. *J. Am. Chem. Soc.* **1997**, *119*, 8403–8408. (b) Lin, Y.-J.; Chang, C.-H.; Horng, J.-C. The Impact of 4-Thiaproline on Polyproline Conformation. *J. Phys. Chem. B* **2014**, *118*, 10813–10820. (c) Goodman, M.; Su, K.-C.; Niu, G. C. C.

- Conformational aspects of polypeptide structure. XXXII. Helical poly[(S)-thiazolidine-4-carboxylic acid]. Experimental results. J. Am. Chem. Soc. 1970, 92, 5220-5222. (d) Frans; Borremans, A. M.; Nachtergaele, W. A.; Budesinsky, M.; Marc; Anteunis, J. O.; Kozodziejczyk, A.; Liberek, B. Solution Conformation of Cis and Trans N-Acetyl-L-Thiazolidine-4-Carboxylic Acid. Bull. Soc. Chim. Belg. 2010, 89, 101-112. (e) Dumy, P.; Keller, M.; Ryan, D. E.; Rohwedder, B.; Wöhr, T.; Mutter, M. Pseudo-Prolines as a Molecular Hinge: Reversible Induction of cis Amide Bonds into Peptide Backbones. J. Am. Chem. Soc. 1997, 119, 918-925. (f) Keller, M.; Sager, C.; Dumy, P.; Schutkowski, M.; Fischer, G. S.; Mutter, M. Enhancing the Proline Effect: Pseudo-Prolines for Tailoring Cis/ Trans Isomerization. J. Am. Chem. Soc. 1998, 120, 2714-2720. (g) Che, Y.; Marshall, G. R. Impact of Cis-proline analogs on peptide conformation. Biopolymers 2006, 81, 392-406. (h) Kang, Y. K.; Park, H. S.; Byun, B. J. Puckering transitions of pseudoproline residues. Biopolymers 2009, 91, 444-455. (i) Choudhary, A.; Pua, K. H.; Raines, R. T. Quantum mechanical origin of the conformational preferences of 4-thiaproline and its S-oxides. Amino Acids 2011, 41, 181-186.
- (7) Aronoff, M. R.; Egli, J.; Menichelli, M.; Wennemers, H. γ-Azaproline Confers pH Responsiveness and Functionalizability on Collagen Triple Helices. *Angew. Chem., Int. Ed.* **2019**, 58, 3143–3146. (8) (a) Martin, C.; Legrand, B.; Lebrun, A.; Berthomieu, D.; Martinez, J.; Cavelier, F. Silaproline Helical Mimetics Selectively Form an All-trans PPII Helix. *Chem.—Eur. J.* **2014**, 20, 14240–14244. (b) Cavelier, F.; Vivet, B.; Martinez, J.; Aubry, A.; Didierjean, C.; Vicherat, A.; Marraud, M. Influence of Silaproline on Peptide Conformation and Bioactivity. *J. Am. Chem. Soc.* **2002**, 124, 2917–2923. (c) Vivet, B.; Cavelier, F.; Martinez, J. Synthesis of Silaproline, a New Proline Surrogate. *Eur. J. Org. Chem.* **2000**, 2000, 807–811.
- (9) Zhang, Y.; Malamakal, R. M.; Chenoweth, D. M. A Single Stereodynamic Center Modulates the Rate of Self-Assembly in a Biomolecular System. *Angew. Chem., Int. Ed.* **2015**, *54*, 10826–10832. (10) (a) Sarnowski, M. P.; Kang, C. W.; Elbatrawi, Y. M.; Wojtas, L.; Del Valle, J. R. Peptide N-Amination Supports  $\beta$ -Sheet Conformations. *Angew. Chem., Int. Ed.* **2017**, *56*, 2083–2086. (b) Kang, C. W.; Sarnowski, M. P.; Elbatrawi, Y. M.; Del Valle, J. R. Access to Enantiopure  $\alpha$ -Hydrazino Acids for N-Amino Peptide Synthesis. *J. Org. Chem.* **2017**, *82*, 1833–1841.
- (11) Alemán, C. N-Amination of Peptides: A Theoretical Study. J. Phys. Chem. A 2002, 106, 1441-1449.
- (12) Knapp, S.; Toby, B. H.; Sebastian, M.; Krogh-Jespersen, K.; Potenza, J. A. Relative Reactivity and Structures of Benzoyltrimethylhydrazine and 1-Benzoyl-2-Methylpyrazolidine. *J. Org. Chem.* **1981**, *46*, 2490–2497.
- (13) (a) Hanessian, S.; Reinhold, U.; Gentile, G. The Synthesis of Enantiopure  $\omega$ -Methanoprolines and  $\omega$ -Methanopipecolic Acids by a Novel Cyclopropanation Reaction: The "Flattering" of Proline. Angew. Chem., Int. Ed. Engl. 1997, 36, 1881-1884. (b) Flores-Ortega, A.; Casanovas, J.; Zanuy, D.; Nussinov, R.; Alemán, C. Conformations of Proline Analogues Having Double Bonds in the Ring. J. Phys. Chem. B 2007, 111, 5475-5482. (c) Kubyshkin, V.; Budisa, N. cis-trans-Amide isomerism of the 3,4-dehydroproline residue, the 'unpuckered' proline. Beilstein J. Org. Chem. 2016, 12, 589-593. (d) Kang, Y. K.; Park, H. S. Conformational preferences and cis-trans isomerization of L-3,4-dehydroproline residue. Biopolymers 2009, 92, 387-398. (e) Matsui, S.; Srivastava, V. P.; Holt, E. M.; Taylor, E. W.; Stammer, C. H. Synthesis and conformational analysis of l-aspartylproline and l-aspartyl-2,3-methanoproline propyl esters. Int. J. Pept. Protein Res. 2009, 37, 306-314. (f) Jeannotte, G.; Lubell, W. D. Large Structural Modification with Conserved Conformation: Analysis of  $\Delta 3$ -Fused Aryl Prolines in Model  $\beta$ -Turns. J. Am. Chem. Soc. **2004**, 126, 14334–14335.
- (14) (a) Magnin, D. R.; Robl, J. A.; Sulsky, R. B.; Augeri, D. J.; Huang, Y.; Simpkins, L. M.; Taunk, P. C.; Betebenner, D. A.; Robertson, J. G.; Abboa-Offei, B. E.; Wang, A.; Cap, M.; Xin, L.; Tao, L.; Sitkoff, D. F.; Malley, M. F.; Gougoutas, J. Z.; Khanna, A.; Huang, Q.; Han, S.-P.; Parker, R. A.; Hamann, L. G. Synthesis of Novel

Potent Dipeptidyl Peptidase IV Inhibitors with Enhanced Chemical Stability: Interplay between the N-Terminal Amino Acid Alkyl Side Chain and the Cyclopropyl Group of α-Aminoacyl-l-cis-4,5-methanoprolinenitrile-Based Inhibitors. *J. Med. Chem.* **2004**, 47, 2587–2598. (b) Augeri, D. J.; Robl, J. A.; Betebenner, D. A.; Magnin, D. R.; Khanna, A.; Robertson, J. G.; Wang, A.; Simpkins, L. M.; Taunk, P.; Huang, Q.; Han, S.-P.; Abboa-Offei, B.; Cap, M.; Xin, L.; Tao, L.; Tozzo, E.; Welzel, G. E.; Egan, D. M.; Marcinkeviciene, J.; Chang, S. Y.; Biller, S. A.; Kirby, M. S.; Parker, R. A.; Hamann, L. G. Discovery and Preclinical Profile of Saxagliptin (BMS-477118): A Highly Potent, Long-Acting, Orally Active Dipeptidyl Peptidase IV Inhibitor for the Treatment of Type 2 Diabetes. *J. Med. Chem.* **2005**, 48, 5025–5037.

(15) For selected examples, see: (a) Hennessy, E. J.; Adam, A.; Aquila, B. M.; Castriotta, L. M.; Cook, D.; Hattersley, M.; Hird, A. W.; Huntington, C.; Kamhi, V. M.; Laing, N. M.; Li, D.; MacIntyre, T.; Omer, C. A.; Oza, V.; Patterson, T.; Repik, G.; Rooney, M. T.; Saeh, J. C.; Sha, L.; Vasbinder, M. M.; Wang, H.; Whitston, D. Discovery of a Novel Class of Dimeric Smac Mimetics as Potent IAP Antagonists Resulting in a Clinical Candidate for the Treatment of Cancer (AZD5582). J. Med. Chem. 2013, 56, 9897-9919. (b) Maibaum, J.; Liao, S.-M.; Vulpetti, A.; Ostermann, N.; Randl, S.; Rüdisser, S.; Lorthiois, E.; Erbel, P.; Kinzel, B.; Kolb, F. A.; Barbieri, S.; Wagner, J.; Durand, C.; Fettis, K.; Dussauge, S.; Hughes, N.; Delgado, O.; Hommel, U.; Gould, T.; Mac Sweeney, A.; Gerhartz, B.; Cumin, F.; Flohr, S.; Schubart, A.; Jaffee, B.; Harrison, R.; Risitano, A. M.; Eder, J.; Anderson, K. Small-molecule factor D inhibitors targeting the alternative complement pathway. Nat. Chem. Biol. 2016, 12, 1105-1110. (c) Abrahamsson, K.; Andersson, P.; Bergman, J.; Bredberg, U.; Brånalt, J.; Egnell, A.-C.; Eriksson, U.; Gustafsson, D.; Hoffman, K.-J.; Nielsen, S.; Nilsson, I.; Pehrsson, S.; Polla, M. O.; Skjaeret, T.; Strimfors, M.; Wern, C.; Ölwegård-Halvarsson, M.; Örtengren, Y. Discovery of AZD8165-a clinical candidate from a novel series of neutral thrombin inhibitors. MedChemComm 2016, 7, 272-281. (d) Venkatraman, S.; Bogen, S. L.; Arasappan, A.; Bennett, F.; Chen, K.; Jao, E.; Liu, Y.-T.; Lovey, R.; Hendrata, S.; Huang, Y.; Pan, W.; Parekh, T.; Pinto, P.; Popov, V.; Pike, R.; Ruan, S.; Santhanam, B.; Vibulbhan, B.; Wu, W.; Yang, W.; Kong, J.; Liang, X.; Wong, J.; Liu, R.; Butkiewicz, N.; Chase, R.; Hart, A.; Agrawal, S.; Ingravallo, P.; Pichardo, J.; Kong, R.; Baroudy, B.; Malcolm, B.; Guo, Z.; Prongay, A.; Madison, V.; Broske, L.; Cui, X.; Cheng, K.-C.; Hsieh, Y.; Brisson, J.-M.; Prelusky, D.; Korfmacher, W.; White, R.; Bogdanowich-Knipp, S.; Pavlovsky, A.; Bradley, P.; Saksena, A. K.; Ganguly, A.; Piwinski, J.; Girijavallabhan, V.; Njoroge, F. G. Discovery of (1R,5S)-N-[3-Amino-1-(cyclobutylmethyl)-2,3-dioxopropyl]- 3-[2(S)-[[(1,1-dimethylethyl)amino]carbonyl]amino]-3,3-dimethyl-1-oxobutyl]- 6,6-dimethyl-3azabicyclo[3.1.0]hexan-2(S)-carboxamide (SCH 503034), a Selective, Potent, Orally Bioavailable Hepatitis C Virus NS3 Protease Inhibitor: A Potential Therapeutic Agent for the Treatment of Hepatitis C Infection. J. Med. Chem. 2006, 49, 6074-6086.

(16) (a) Mauger, A. B. Naturally occurring proline analogues. *J. Nat. Prod.* **1996**, *59*, 1205–1211. (b) Li, W.; Estrada-de los Santos, P.; Matthijs, S.; Xie, G.-L.; Busson, R.; Cornelis, P.; Rozenski, J.; De Mot, R. Promysalin, a Salicylate-Containing Pseudomonas putida Antibiotic, Promotes Surface Colonization and Selectively Targets Other Pseudomonas. *Chem. Biol.* **2011**, *18*, 1320–1330.

(17) (a) Zhang, R.; Madalengoitia, J. S. Design, Synthesis and Evaluation of Poly-l-Proline Type-II Peptide Mimics Based on the 3-Azabicyclo[3.1.0]hexane System. J. Org. Chem. 1999, 64, 330–331. (b) Priem, C.; Geyer, A. Synthetic Marine Sponge Collagen by Late-Stage Dihydroxylation. Org. Lett. 2018, 20, 162–165. (c) Rosenbloom, J.; Prockop, D. J. Incorporation of 3,4-Dehydroproline into Protocollagen and Collagen: Limited hydroxylation of proline and lysine in the same polypeptide. J. Biol. Chem. 1970, 245, 3361–8. (d) Zhao, Z.; Liu, X.; Shi, Z.; Danley, L.; Huang, B.; Jiang, R.-T.; Tsai, M.-D. Mechanism of Adenylate Kinase. 20. Probing the Importance of the Aromaticity in Tyrosine-95 and the Ring Size in Proline-17 with Unnatural Amino Acids. J. Am. Chem. Soc. 1996, 118, 3535–3536.

- (18) (a) Duttagupta, I.; Misra, D.; Bhunya, S.; Paul, A.; Sinha, S. Cis-Trans Conformational Analysis of  $\delta$ -Azaproline in Peptides. I. Org. Chem. 2015, 80, 10585-10604. (b) Humbert-Voss, E.; Arrault, A.; Jamart-Grégoire, B. Synthesis and conformational behavior of pseudopeptides containing  $\delta$ -azaproline. A cis conformational preference for Xaa1 $-\delta$ -azaPro bond. *Tetrahedron* **2014**, 70, 363-370. (19) (a) Xi, N.; Alemany, L. B.; Ciufolini, M. A. Elevated Conformational Rigidity in Dipeptides Incorporating Piperazic Acid Derivatives. J. Am. Chem. Soc. 1998, 120, 80-86. (b) Ciufolini, M. A.; Xi, N. Synthesis, chemistry and conformational properties of piperazic acids. Chem. Soc. Rev. 1998, 27, 437-445. (c) Wu, W.-J.; Raleigh, D. P. Conformational Heterogeneity about Pipecolic Acid Peptide Bonds: Conformational, Thermodynamic, and Kinetic Aspects. J. Org. Chem. 1998, 63, 6689-6698. (d) Howard, E. H.; Cain, C. F.; Kang, C.; Del Valle, J. R. Synthesis of Enantiopure  $\varepsilon$ -Oxapipecolic Acid. J. Org. Chem. 2020, 85, 1680. , In press
- (20) Derivatives in which a *trans* amide geometry was enforced through covalent tethering were not included in this analysis.
- (21) Shireman, B. T.; Miller, M. J.; Jonas, M.; Wiest, O. Conformational Study and Enantioselective, Regiospecific Syntheses of Novel Aminoxy trans-Proline Analogues Derived from an Acylnitroso Diels-Alder Cycloaddition. *J. Org. Chem.* **2001**, *66*, 6046–6056.
- (22) (a) Voss, E.; Arrault, A.; Bodiguel, J.; Jamart-Grégoire, B. Efficient synthesis of enantiomerically pure (S)- $\delta$ -azaproline starting from (R)- $\alpha$ -hydroxy- $\gamma$ -butyrolactone via the Mitsunobu reaction. *Tetrahedron: Asymmetry* **2009**, 20, 1809–1812. (b) Kim, H.-O.; Lum, C.; Lee, M. S. Malic acid: A convenient precursor for the synthesis of peptide secondary structure mimetics. *Tetrahedron Lett.* **1997**, 38, 4935–4938.
- (23) Mish, M. R.; Guerra, F. M.; Carreira, E. M. Asymmetric Dipolar Cycloadditions of Me3SiCHN2. Synthesis of a Novel Class of Amino Acids: Azaprolines. *J. Am. Chem. Soc.* **1997**, *119*, 8379–8380.
- (24) Kline, T.; Andersen, N. H.; Harwood, E. A.; Bowman, J.; Malanda, A.; Endsley, S.; Erwin, A. L.; Doyle, M.; Fong, S.; Harris, A. L.; Mendelsohn, B.; Mdluli, K.; Raetz, C. R. H.; Stover, C. K.; Witte, P. R.; Yabannavar, A.; Zhu, S. Potent, Novel in Vitro Inhibitors of the Pseudomonas aeruginosa Deacetylase LpxC. *J. Med. Chem.* **2002**, *45*, 3112–3129.
- (25) Armstrong, A.; Jones, L. H.; Knight, J. D.; Kelsey, R. D. Oxaziridine-Mediated Amination of Primary Amines: Scope and Application to a One-Pot Pyrazole Synthesis. *Org. Lett.* **2005**, *7*, 713–716
- (26) Dekan, Z.; Vetter, I.; Daly, N. L.; Craik, D. J.; Lewis, R. J.; Alewood, P. F.  $\alpha$ -Conotoxin ImI Incorporating Stable Cystathionine Bridges Maintains Full Potency and Identical Three-Dimensional Structure. *J. Am. Chem. Soc.* **2011**, *133*, 15866–15869.
- (27) Greenberg, J. A.; Sammakia, T. The Conversion of tert-Butyl Esters to Acid Chlorides Using Thionyl Chloride. *J. Org. Chem.* **2017**, 82, 3245–3251.
- (28) A weak  $H\alpha$ -Me<sub>amide</sub> correlation (disproportionately small relative to  $H\alpha$ -H $\beta$  correlations) is observed due to distance that is within the threshold for NOE. This correlation is similar in magnitude to that of the  $H\alpha$ -Me<sub>ester</sub> correlation, indicating an equivalent interatomic distance and a *trans* amide geometry.
- (29) Che, Y.; Marshall, G. R. Impact of Azaproline on Peptide Conformation. J. Org. Chem. 2004, 69, 9030–9042.
- (30) See the Supporting Information for details.
- (31) Rai, R.; Raghothama, S.; Balaram, P. Design of a Peptide Hairpin Containing a Central Three-Residue Loop. *J. Am. Chem. Soc.* **2006**, *128*, 2675–2681.
- (32) McDermott, J. R.; Benoiton, N. L. N-Methylamino Acids in Peptide Synthesis. IV. Racemization and Yields in Peptide-bond Formation. *Can. J. Chem.* **1973**, *51*, 2562–2570.
- (33) Berger, G.; Vilchis-Reyes, M.; Hanessian, S. Structural Properties and Stereochemically Distinct Folding Preferences of 4,5-cis and trans-Methano-L-Proline Oligomers: The Shortest Crystalline PPII-Type Helical Proline-Derived Tetramer. *Angew. Chem., Int. Ed.* **2015**, 54, 13268–13272.

(34) (a) Kaduskar, R. D.; Dhavan, A. A.; Dallavalle, S.; Scaglioni, L.; Musso, L. Total synthesis of the salicyldehydroproline-containing antibiotic promysalin. *Tetrahedron* **2016**, 72, 2034–2041. (b) Steele, A. D.; Keohane, C. E.; Knouse, K. W.; Rossiter, S. E.; Williams, S. J.; Wuest, W. M. Diverted Total Synthesis of Promysalin Analogs Demonstrates That an Iron-Binding Motif Is Responsible for Its Narrow-Spectrum Antibacterial Activity. *J. Am. Chem. Soc.* **2016**, 138, 5833–5836.